Theoretical Insights into In-context Learning with Unlabeled Data

Anonymous Authors[1]

Abstract

Recent research shows that in-context learning (ICL) can be effective even in settings where demonstrations have missing or incorrect labels. This motivates a deeper understanding of how sequence models leverage unlabeled data. We consider a canonical setting where the in-context demonstrations are drawn according to a binary Gaussian mixture model (GMM) and a certain fraction of the demonstrations have missing labels. We provide a comprehensive theoretical study to show that: (1) The loss landscape of one-layer linear attention learns the optimal fully-supervised learner but it completely fails to leverage the unlabeled data. (2) Multilayer as well as looped transformers can effectively leverage unlabeled data by implicitly constructing estimators of the form $\sum_{i\geq 0} a_i(\boldsymbol{X}^\top \boldsymbol{X})^i \boldsymbol{X}^\top \boldsymbol{y}$ with $\boldsymbol{X}$ and $\boldsymbol{y}$ denoting features and visible labels. We shed light on the class of polynomials that can be expressed as a function of depth/looping and draw connections to iterative pseudo-labeling.

1. Introduction

In-Context Learning (ICL) is an intriguing capability of modern language models and has enjoyed remarkable empirical success (Brown et al., 2020; Min et al., 2022). The push toward long-context models (Snell et al., 2024; Guo et al., 2025) has further boosted the benefits of ICL by allowing the model to ingest a large number of demonstrations. For instance, in "Many-shot in-context learning" paper, (Agarwal et al., 2024) demonstrate that pushing more examples into context window can substantially boost the accuracy. The many-shot ICL setting naturally raises the question of when and how ICL can succeed with weaker supervision. This motivates our central question:

***Q:** How can transformers learn from unlabeled data?*

We primarily investigate this question under a semisupervised ICL (SS-ICL) setting with GMMs. Formally, given a prompt containing a dataset of feature-label pairs $(\boldsymbol{x}_i, y_i)_{i=1}^n \in \mathbb{R}^d \times \mathbb{R}$ as demonstrations and a query feature $\boldsymbol{x}$, a model learns to predict the corresponding output y given prompt. This prompt model is well studied under various fully-supervised settings (Garg et al., 2022; Von Oswald et al., 2023; Ahn et al., 2023; Akyürek et al., 2023; Mahankali et al., 2024; Collins et al., 2024; Shen et al., 2024) where each demonstration includes a clearly labeled output. In our SS-ICL setting, only m out of n total samples have correct labels ($m \leq n$) either -1 or 1, and remaining labels are unknown and fed to the model as $y_i = 0$.

In this work, we provide a comprehensive theoretical and empirical study of attention models with varying depths when trained with SS-ICL. Our analysis reveals **the importance of depth**: despite being able to implement the optimal supervised learner, single-layer linear attention completely fails to leverage unlabeled examples. In contrast, deeper or looped transformer architectures can emulate strong semi-supervision algorithms. Our specific contributions are:

- **Landscape of one-layer linear attention (§3):** We study the optimization landscape of single-layer linear attention for the SS-ICL problem under an isotropic task prior. We prove that the global minimum of the loss function is the plug-in estimator (cf. (SPI)). This implies that 1-layer model learns Bayes-optimal classifier in the fully-supervised setting, but completely fails to make use of unlabeled data.
- **Depth is crucial but shallow can suffice (§4):** We show that multilayer linear attention can emulate semisupervised learners by implementing polynomial estimators of the form $\hat{\boldsymbol{\mu}} = \sum_{i\geq 0}^{K} a_i(\boldsymbol{X}^\top \boldsymbol{X})^i \boldsymbol{X}^\top \boldsymbol{y}$, which can be interpreted as the model implicitly conducting *iterative pseudo-labeling*. We show that L-layer (or looped) attention can express up to $K = O(3^L)$ powers, highlighting exponentiation requires only logarithmic depth. Corroborating these, experiments reveal that shallow transformers with $L \geq 2$ already achieve strong results and their performance can be approximately predicted through an eigen-estimator combining $i = 0$ and ∞ (see (SSPI-k)).
- **Applications to Tabular FMs (§B):** Tabular foundation models such as TabPFN (Hollmann et al., 2022;

[1]Anonymous Institution, Anonymous City, Anonymous Region, Anonymous Country. Correspondence to: Anonymous Author <anon.email@domain.com>.

Preliminary work. Under review by the International Conference on Machine Learning (ICML). Do not distribute.

2025) and TabICL (Qu et al., 2025) represent a suitable application of theory as they also model the ICL examples with a single token. To harness unlabeled examples, we propose a novel strategy that iteratively creates soft pseudo-labels by *explicitly looping the tabular FM* while controlling validation risk. Focusing on the few-shot learning setting where TabPFN-v2 excels, we demonstrate that our approach can significantly improve performance on various real-world datasets. Experiments are detailed in Appendix B and F.

2. Problem Setup and Preliminaries

2.1. Semi-supervised Data Model

Consider a d-dimensional semi-supervised binary GMM with n examples $(\boldsymbol{x}_i, y_i)_{i=1}^n$, where $\boldsymbol{x}_i \in \mathbb{R}^d$ denotes the feature vector and $y_i \in \{-1, 0, 1\}$ represents the corresponding observed label, with $y_i = 0$ indicating a missing label, and each label is revealed independently with probability $p \in [0, 1]$. Specifically, the data is generated as follows (for each $i \in [n]$):

$$\boldsymbol{x}_i = y_i^c \cdot \boldsymbol{\mu} + \boldsymbol{\xi}_i \quad \text{and} \quad y_i = \begin{cases} y_i^c, & \text{w.p.} \quad p \\ 0, & \text{w.p.} \quad 1-p \end{cases} \tag{1}$$

where $\boldsymbol{y}_i^c \sim$ Unif{1,-1} denotes the true label. Here $\boldsymbol{\mu} \sim \text{Unif}(\mathbb{S}^{d-1})$ denotes the task mean, which is sampled uniformly from the unit sphere, and $\boldsymbol{\xi}_i \sim \mathcal{N}(0, \sigma^2 \boldsymbol{I})$ is the random noise with $\sigma \geq 0$ being the noise level that controls the variability of $\boldsymbol{x}_i$ around its mean. Observe that $p = 1$ corresponds to fully supervised learning and $p = 0$ corresponds to fully-unsupervised learning.

2.2. In-context Learning and Linear Attention

We build on the setting of (Garg et al., 2022; Mahankali et al., 2024; Zhang et al., 2023; Li et al., 2024) and construct the in-context prompts with examples drawn from (1).

Prompt Generation: Given a task vector $\boldsymbol{\mu} \sim \text{Unif}(\mathbb{S}^{d-1})$, we sample $(n+1)$ in-context demonstrations $(\boldsymbol{x}_i, y_i)_{i=1}^{n+1}$ according to (1) and construct the prompt

$$\boldsymbol{Z} = \begin{bmatrix} \boldsymbol{x}_1 & \boldsymbol{x}_2 & \cdots & \boldsymbol{x}_n & \boldsymbol{x} \\ y_1 & y_2 & \cdots & y_n & 0 \end{bmatrix}^\top \in \mathbb{R}^{(n+1)\times(d+1)}. \tag{2}$$

We will investigate training a transformer such that given $\boldsymbol{Z}$ as prompt, it correctly predicts the label $\boldsymbol{y} := y_{n+1}^c$ of the query $\boldsymbol{x} := \boldsymbol{x}_{n+1}$ through ICL.

Model Architecture: Given any prompt $\boldsymbol{Z} \in \mathbb{R}^{(n+1)\times(d+1)}$, the linear attention mechanism outputs

$$\text{att}(\boldsymbol{Z}; \mathcal{W}) = (\boldsymbol{Z}\boldsymbol{W}_q\boldsymbol{W}_k^\top\boldsymbol{Z}^\top)\boldsymbol{M}\boldsymbol{Z}\boldsymbol{W}_v \tag{3}$$

where $\mathcal{W} := \{\boldsymbol{W}_k, \boldsymbol{W}_q, \boldsymbol{W}_v \in \mathbb{R}^{(d+1)\times(d+1)}\}$ denotes the key, query and value weight matrices, respectively. Note that the label for the query $\boldsymbol{x}$ is excluded from the prompt $\boldsymbol{Z}$. Similar to Ahn et al. (2023), we consider a training objective with a mask $\boldsymbol{M} = \begin{bmatrix} \boldsymbol{I}_n & 0 \\ 0 & 0 \end{bmatrix}$ to ensure inputs cannot attend to their own labels and training can be parallelized.

Building upon the single-layer linear attention mechanism of (3), we can extend our model to multiple layers to capture more complex patterns. Consider optimizing an L-layer linear attention model and let $\boldsymbol{Z}_\ell$ be the input of ℓth layer, $\ell \in [L]$. Additionally, let $\mathcal{W}_\ell := \{\boldsymbol{W}_{k\ell}, \boldsymbol{W}_{q\ell}, \boldsymbol{W}_{v\ell} \in \mathbb{R}^{(d+1)\times(d+1)}\}$ be the corresponding weight matrices of ℓth layer. Then, the input prompt of ℓth layer is defined by

$$\boldsymbol{Z}_\ell = \boldsymbol{Z}_{\ell-1} + \text{att}(\boldsymbol{Z}_{\ell-1}; \mathcal{W}_{\ell-1}) \quad \text{for} \quad \ell = 2, \dots L,$$

and $\boldsymbol{Z}_1 = \boldsymbol{Z}$. We focus on the next-token prediction setting, where the model makes a prediction based on the final query token $[\boldsymbol{x}^\top \; 0]^\top$. Let $\boldsymbol{h} \in \mathbb{R}^{d+1}$ denote the linear prediction head. We define the output of the L-layer linear attention model at the last (query) token as

$$f_{\text{att-}L}(\boldsymbol{Z}) = \boldsymbol{h}^\top \text{att}(\boldsymbol{Z}_L; \mathcal{W}_L)_{[n+1]}. \tag{4}$$

The predicted label is given by $y_{\text{att-}L}(\boldsymbol{Z}) = \text{sgn}(f_{\text{att-}L}(\boldsymbol{Z}))$.

Model Training: Consider the ICL setting where each input prompt $\boldsymbol{Z}$ (cf. (2)) corresponds to a randomly sampled task vector $\boldsymbol{\mu} \sim \text{Unif}(\mathbb{S}^{d-1})$ and let $\ell(\cdot) : \mathbb{R} \to \mathbb{R}$ be the loss function. Additionally, define the set of attention weights $\mathcal{W}^{(L)} := \cup_{\ell=1}^L \mathcal{W}_\ell \in (\mathbb{R}^{(d+1)\times(d+1)})^{3L}$. The objective of L-layer linear atention takes the following form:

$$\min_{\mathcal{W}^{(L)}, \boldsymbol{h}} \mathcal{L}_{\text{att-}L}(\mathcal{W}^{(L)}, \boldsymbol{h}) \tag{5}$$
$$\text{where} \quad \mathcal{L}_{\text{att-}L}(\mathcal{W}^{(L)}, \boldsymbol{h}) = \mathbb{E}\left[\ell(y, f_{\text{att-}L}(\boldsymbol{Z}))\right].$$

Here, $y := y_{n+1}^c$ and the expectation subsumes the randomness of $\boldsymbol{\mu}$ and $(\boldsymbol{\xi}_i, y_i)_{i=1}^{n+1}$.

3. Loss Landscape of One-layer Linear Attention under SS-ICL

In this section, we analyze the optimization behavior of single-layer linear attention under SS-ICL, and demonstrate that the single-layer model learns the optimal fully-supervised learner, but fails to utilize the unlabeled data. We begin with the following optimal supervised label estimator.

Supervised Plug-in (SPI) Estimator: Under our problem setting, SPI method is the Bayes-optimal estimator given only labeled data (Mignacco et al., 2020; Lelarge & Miolane, 2019). Consider the binary semi-supervised GMM problem described in (1) with dataset $(\boldsymbol{x}_i, y_i)_{i=1}^n$, and let $\mathcal{I} \subset [n]$ represent the indices of labeled samples, e.g., $y_i \neq 0$ for $i \in \mathcal{I}$. The SPI estimator returns the task mean

$$\hat{\boldsymbol{\mu}}_s = \frac{1}{|\mathcal{I}|} \sum_{i \in \mathcal{I}} y_i \boldsymbol{x}_i. \tag{SPI}$$

Theorem 3.1. *Consider the objective (cf. (5)) with $L = 1$ and squared loss function $\ell(y, \hat{y}) = (y - \hat{y})^2$, and denote the optimal prediction as $y^\star_{\text{att-1}}(\boldsymbol{Z})$. Let $\hat{\boldsymbol{\mu}}_s$ represent the SPI estimator defined in (SPI). Then, for any $\boldsymbol{Z}$ from (2),*

$$y^\star_{\text{att-1}}(\boldsymbol{Z}) = sgn(\boldsymbol{x}^\top \hat{\boldsymbol{\mu}}_s). \tag{6}$$

Additionally, its classification error obeys $\mathbb{P}(y^\star_{\text{att-1}}(\boldsymbol{Z}) \neq y)$

$$= \mathbb{E}_{g\sim\mathcal{N}(0,1), h\sim\mathcal{X}^2_{d-1}}\left[Q\left(\frac{1+\varepsilon_\sigma g}{\sigma\sqrt{(1+\varepsilon_\sigma g)^2 + \varepsilon_\sigma^2 h}}\right)\right] \tag{7}$$

$$\leq Q\left(\frac{1-10d\varepsilon_\sigma^2}{\sigma}\right) + e^{-d} + e^{-1/8\varepsilon_\sigma^2}.$$

where we define $\varepsilon_\sigma = \sigma/\sqrt{np}$ and $\mathcal{X}^2_d$ defines chi-squared distribution with d degrees of freedom.

Eq. (6) shows that one-layer linear attention model indeed implements SPI predictor, assuming access to np labeled examples. Most existing work (Thrampoulidis et al., 2020; Wang & Thrampoulidis, 2022) focuses on a single classification task under asymptotic data regimes. In contrast, within the ICL framework considered in our setting, the task mean $\boldsymbol{\mu}$ is randomly sampled, and the classification error is computed by averaging over random draws of $\boldsymbol{Z}$, y, and $\boldsymbol{\mu}$. Accordingly, in (7), we express the error in a simplified form as an expectation.

The experimental results in Figure 1 support Theorem 3.1, where dark blue circular markers represent the performance of the single-layer linear attention model, blue curves show the classification accuracy of the SPI estimator, and the red dotted curves depict $1-\mathbb{P}(y^\star_{\text{att-1}}(\boldsymbol{Z}) \neq y)$ as computed from (7). The alignments of these curves empirically validate Theorem 3.1. Based on these results, we can conclude: *1-layer linear attention learns optimal supervised estimator but doesn't benefit from unlabeled data.*

As shown in Figs 1(b) and 1(c), when the number of labeled samples ($np = 10$) is fixed, increasing the number of unlabeled examples (even up to ~ 10000) has no effect on performance, as the dark blue markers remain at the same level. At first glance, this may seem counterintuitive—while the data is unlabeled, it still contains information about the classification feature. For instance, the mean of the data points carries relevant information, and one might expect the model to extract and leverage this for better predictions. This expectation is particularly reasonable when a large amount of unlabeled data is available, as the sample covariance matrix approximates the population covariance, i.e., $\mathbb{E}[\boldsymbol{X}^\top\boldsymbol{X}/n] = \boldsymbol{\mu}\boldsymbol{\mu}^\top + \sigma^2\boldsymbol{I}$ where $\boldsymbol{X} = [\boldsymbol{x}_1, \boldsymbol{x}_2, \cdots, \boldsymbol{x}_n]^\top \in \mathbb{R}^{n\times d}$. The key insight into why single-layer attention fails to leverage unlabeled data lies in the expectation structure. In our isotropic GMM setting where $\boldsymbol{\mu} \sim \text{Unif}(\mathbb{S}^{d-1})$, the sample covariance matrix converges to $\mathbb{E}[\boldsymbol{X}^\top\boldsymbol{X}/n] = \mathbb{E}[\boldsymbol{\mu}\boldsymbol{\mu}^\top] + \sigma^2\boldsymbol{I} = (1/d + \sigma^2)\boldsymbol{I}$, which contains no task-specific information. The expectation across multiple tasks loses the signal from $\boldsymbol{\mu}$. This explains why single-layer attention, operating in a meta-learning framework across many tasks rather than optimizing for a single fixed task, cannot extract useful information from unlabeled data.

In the following section, we study multi-layer linear attention and demonstrate that it has the ability to propagate $\boldsymbol{X}^\top\boldsymbol{X}$ into deeper layers, thereby enabling the model to utilize the unlabeled data.

4. Multi-layer Attention and the Benefits of Depth

In this section, we explore how deeper attention models can effectively utilize the unlabeled data. Let

$$\boldsymbol{X} = \begin{bmatrix}\boldsymbol{x}_1 & \cdots & \boldsymbol{x}_n\end{bmatrix}^\top \text{ and } \boldsymbol{y} = \begin{bmatrix}y_1 & \cdots & y_n\end{bmatrix}^\top. \tag{8}$$

We first present the following propositions to show that multi-layer as well as looped linear attention can be expressed as a polynomial function of $\boldsymbol{X}^\top\boldsymbol{X}$. This structure allows the models to leverage unlabeled data to improve the estimation of the task mean $\boldsymbol{\mu}$.

Proposition 4.1. *Given an L-layer linear attention model described in Section 2.2 with input prompt $\boldsymbol{Z}$ defined in (2), one can construct the key, query, value weight matrices and the linear prediction head such that the model outputs*

$$f_{\text{att-}L}(\boldsymbol{Z}) = \boldsymbol{x}^\top\boldsymbol{A}\boldsymbol{X}^\top\boldsymbol{y}. \tag{9}$$

Then, the following $\boldsymbol{A}$ matrices are achievable:

- ***Label propagation:*** *$\boldsymbol{A} = c\prod_{\ell=1}^{L-1}\left(\boldsymbol{I} + c_\ell\boldsymbol{X}^\top\boldsymbol{X}\right)$ for arbitrary constants $\{c, c_1, \cdots, c_{L-1}\}$;*
- ***Feature propagation:*** *$\boldsymbol{A} = c\left(\boldsymbol{X}^\top\boldsymbol{X}\right)^{3^{L-1}-1}$ for an arbitrary constant c.*

Proposition 4.2. *Consider the same setting as in Proposition 4.1. There exists a single-layer linear attention model whose parameters can be constructed to reproduce the output in (9), with $c_\ell \equiv c'$ for some arbitrary constant c'.*

In the following, we provide further clarification on the label and feature propagation.

1. The final prediction of the label propagation process can be rewritten as (for $\ell \in [L-1]$)

   $$f_{\text{att-}L}(\boldsymbol{Z}) = c\boldsymbol{x}^\top\boldsymbol{X}^\top\boldsymbol{y}_L \text{ where } \boldsymbol{y}_{\ell+1} = (\boldsymbol{I} + c_\ell\boldsymbol{X}\boldsymbol{X}^\top)\boldsymbol{y}_\ell,$$

   with $\boldsymbol{y}_1 = \boldsymbol{y}$. Here, $\boldsymbol{y}_\ell$ can be interpreted as the pseudo-labels input to the ℓth layer, and each c_ℓ is parameterized by the attention mechanism in the corresponding layer. The L-layer linear attention process shares similarities with the Expectation-Maximization algorithm for semi-supervised learning, with L iterations of pseudo-labeling and a different label update strategy.

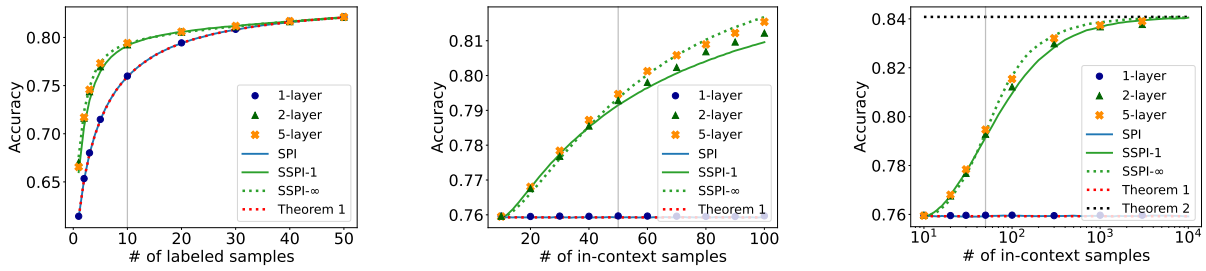

(a) $n = 50, p \in (0, 1]$. (b) $np = 10, n \in \{10, \cdots, 100\}$. (c) $np = 10, n \in \{10, \cdots, 10000\}$.

Figure 1. Experimental results support our theoretical findings presented in Sections 3 and 4.

2. In contrast, the feature propagation process yields

$$f_{\text{all-}L}(\boldsymbol{Z}) = c\boldsymbol{x}_L^\top \boldsymbol{X}_L^\top \boldsymbol{y} \quad \text{where} \quad \begin{cases} \boldsymbol{X}_{\ell+1} = (\boldsymbol{X}_\ell \boldsymbol{X}_\ell^\top)\boldsymbol{X}_\ell \\ \boldsymbol{x}_{\ell+1} = (\boldsymbol{X}_\ell^\top \boldsymbol{X}_\ell)\boldsymbol{x}_\ell \end{cases}$$

with $(\boldsymbol{X}_1, \boldsymbol{x}_1) = (\boldsymbol{X}, \boldsymbol{x})$. Here, $(\boldsymbol{X}_\ell, \boldsymbol{x}_\ell)$ can be viewed as the input features at the ℓth layer, encoding exponentially higher-order powers of $\boldsymbol{X}^\top \boldsymbol{X}$. This result highlights that a linear attention model requires only $O(\log k)$ layers to represent polynomial functions of degree k.

Our construction for *label propagation* is inherently related to the GD emulation capability of linear attention (Ahn et al., 2023). The lemma below shows that, even if the multilayer model can express polynomials of $\boldsymbol{X}^\top \boldsymbol{X}$ with exponential degrees in depth, the expressible manifold of polynomials has dimensionality linear in depth.

Lemma 4.3 (Label + Feature Propagation)**.** *For an L-layer linear attention model, the resulting eventual prediction corresponds to the matrix $\boldsymbol{A}$ in Proposition 4.1 of the form*

$$\boldsymbol{A} = \sum_{\ell=0}^{(3^L-3)/2} a_\ell (\boldsymbol{X}^\top \boldsymbol{X})^\ell. \tag{10}$$

The coefficients $\boldsymbol{a} := [a_0 \ \cdots \ a_{(3^L-3)/2}]^\top$ lie on a manifold of dimension at most $2L$ as $\boldsymbol{a}$ can be expressed as $\boldsymbol{a} = g(\boldsymbol{c})$ for some smooth function $g : \mathbb{R}^{2L} \to \mathbb{R}^{(3^L-3)/2}$ with $\boldsymbol{c}$ representing the parameters of individual layers.

Motivated by Proposition 4.1 that multi-layer linear attention can implement higher-degree polynomials of $\boldsymbol{X}^\top \boldsymbol{X}$, we introduce the following SSPI estimator.

Semisupervised Plug-in (SSPI) Estimator Observe that the feature covariance satisfies $\mathbb{E}[\boldsymbol{X}^\top \boldsymbol{X}]/n = \boldsymbol{\mu}\boldsymbol{\mu}^\top + \sigma^2 \boldsymbol{I}$. We propose the semisupervised plug-in estimator as follows:

$$\hat{\boldsymbol{\mu}}_{ss\text{-}k} = \alpha \hat{\boldsymbol{\mu}}_s + (1-\alpha)(\boldsymbol{X}^\top \boldsymbol{X}/n - \sigma^2 \boldsymbol{I})^k \hat{\boldsymbol{\mu}}_s \quad \text{(SSPI-}k\text{)}$$

where $\hat{\boldsymbol{\mu}}_s$ is the SPI estimator (c.f. (SPI)), and $\alpha \in [0, 1]$ controls the trade-off between the fully-supervised and semi-supervised estimator. The optimal choice of α depends on the problem parameters n, d and p. Note that as $k \to \infty$, the term $(\boldsymbol{X}^\top \boldsymbol{X}/n - \sigma^2 \boldsymbol{I})^k$ converges $\boldsymbol{\mu}\boldsymbol{\mu}^\top$, effectively serving as an estimator for $\boldsymbol{\mu}$ (up to sign).

In Figure 1, we present the prediction accuracies of 2-/5-layer linear attention models, and evaluate the SSPI algorithm with varying k values using their respective optimal choices of α. The results reveal a close alignment between multi-layer linear attention and SSPI estimators. Notably, the 2-layer model outperforms SSPI-1, due to its ability to implement higher-degree polynomials of $\boldsymbol{X}^\top \boldsymbol{X}$ (cf. Proposition 4.1 and (10)). Furthermore, since the 5-layer model is capable of representing higher-order functions than the 2-layer model, it can better estimate the top eigenvector, resulting in performance that closely matches that of SSPI-∞.

In the following, we analyze the optimal classifier of the form $\text{sgn}(\boldsymbol{x}^\top \boldsymbol{A} \hat{\boldsymbol{\mu}}_s)$ for a GMM, and provide insights into its behavior in the asymptotic regime as $n \to \infty$.

Theorem 4.4. *Consider a GMM defined in Section 2.1 and suppose that $(\boldsymbol{x}_i, y_i)_{i=1}^{n+1}$ is generated using a fixed $\boldsymbol{\mu}$ following (1). Given matrix $\boldsymbol{A} \in \mathbb{R}^{d\times d}$, define prediction*

$$\hat{y}_{\boldsymbol{A}} = sgn(\boldsymbol{x}^\top \boldsymbol{A} \hat{\boldsymbol{\mu}}_s).$$

where $\hat{\boldsymbol{\mu}}_s$ is the SPI estimator defined in (SPI). Let $\mathcal{A}^\star := \min_{\boldsymbol{A}\in\mathbb{R}^{d\times d}} \mathbb{P}(\hat{y}_{\boldsymbol{A}} \neq y)$ be its optimal solution set. Then, $\boldsymbol{\mu}\boldsymbol{\mu}^\top \in \mathcal{A}^\star$. Additionally, it obeys $\mathbb{P}(\hat{y}_{\boldsymbol{\mu}\boldsymbol{\mu}^\top} \neq y) =$

$$Q(1/\sigma) + Q(\sqrt{np}/\sigma) - 2Q(1/\sigma)Q(\sqrt{np}/\sigma). \tag{11}$$

Theorem 4.5. *Consider an L-layer linear attention model with $L \geq 2$ and $n = \infty$. Additionally, let $\hat{\boldsymbol{\mu}}_s$ be the SPI estimator defined in (SPI). There exists model constructions such that for any $\boldsymbol{Z}$ following (2), its prediction satisfies*

$$y_{att\text{-}L}(\boldsymbol{Z}) = sgn(\boldsymbol{x}^\top \boldsymbol{\mu}\boldsymbol{\mu}^\top \hat{\boldsymbol{\mu}}_s).$$

The proof follows directly from Proposition 4.1 (label propagation). The results in Figure 1(c) validate Theorem 4.5, showing that as n becomes large enough, (i.e., $n = 10000$) the predictions from both 2-layer and 5-layer linear attention models, as well as the SSPI-1 and SSPI-∞ estimators, closely align with the classification error characterized in Theorem 4.4, depicted by the black dotted line. Non-asymptotic result is presented in Appendix E.5.

References

Agarwal, R., Singh, A., Zhang, L. M., Bohnet, B., Chan, S., Anand, A., Abbas, Z., Nova, A., Co-Reyes, J. D., Chu, E., et al. Many-shot in-context learning. *arXiv preprint arXiv:2404.11018*, 2024.

Ahn, K., Cheng, X., Daneshmand, H., and Sra, S. Transformers learn to implement preconditioned gradient descent for in-context learning. *Advances in Neural Information Processing Systems*, 36, 2023.

Akyürek, E., Schuurmans, D., Andreas, J., Ma, T., and Zhou, D. What learning algorithm is in-context learning? investigations with linear models. In *The Eleventh International Conference on Learning Representations*, 2023. URL https://openreview.net/forum?id=0g0X4H8yN4I.

Balakrishnan, S., Wainwright, M. J., and Yu, B. Statistical guarantees for the EM algorithm: From population to sample-based analysis. In *Annals of Statistics*, volume 45, pp. 77–120. Institute of Mathematical Statistics, 2017.

Brown, T., Mann, B., Ryder, N., Subbiah, M., Kaplan, J. D., Dhariwal, P., Neelakantan, A., Shyam, P., Sastry, G., Askell, A., et al. Language models are few-shot learners. *Advances in neural information processing systems*, 33: 1877–1901, 2020.

Collins, L., Parulekar, A., Mokhtari, A., Sanghavi, S., and Shakkottai, S. In-context learning with transformers: Softmax attention adapts to function lipschitzness. *arXiv preprint arXiv:2402.11639*, 2024.

Dai, D., Sun, Y., Dong, L., Hao, Y., Ma, S., Sui, Z., and Wei, F. Why can GPT learn in-context? language models secretly perform gradient descent as meta-optimizers. In Rogers, A., Boyd-Graber, J., and Okazaki, N. (eds.), *Findings of the Association for Computational Linguistics: ACL 2023*, pp. 4005–4019, Toronto, Canada, July 2023. Association for Computational Linguistics. doi: 10.18653/v1/2023.findings-acl.247. URL https://aclanthology.org/2023.findings-acl.247.

Fan, C., Liu, S., Motamed, S., Zhong, S., Savarese, S., Niebles, J. C., Anandkumar, A., Gaidon, A., and Scherer, S. Expectation maximization pseudo labels. *arXiv preprint arXiv:2305.01747*, 2023.

Garg, S., Tsipras, D., Liang, P. S., and Valiant, G. What can transformers learn in-context? a case study of simple function classes. *Advances in Neural Information Processing Systems*, 35:30583–30598, 2022.

Guo, D., Yang, D., Zhang, H., Song, J., Zhang, R., Xu, R., Zhu, Q., Ma, S., Wang, P., Bi, X., et al. Deepseek-r1: Incentivizing reasoning capability in llms via reinforcement learning. *arXiv preprint arXiv:2501.12948*, 2025.

Hollmann, N., Müller, S., Eggensperger, K., and Hutter, F. Tabpfn: A transformer that solves small tabular classification problems in a second. *arXiv preprint arXiv:2207.01848*, 2022.

Hollmann, N., Müller, S., Purucker, L., Krishnakumar, A., Körfer, M., Hoo, S. B., Schirrmeister, R. T., and Hutter, F. Accurate predictions on small data with a tabular foundation model. *Nature*, 637(8045):319–326, 2025.

Krishnapuram, B., Williams, D., Xue, Y., Carin, L., Figueiredo, M., and Hartemink, A. On semi-supervised classification. *Advances in neural information processing systems*, 17, 2004.

Kumar, A., Engstrom, L., Ilyas, A., and Tsipras, D. Understanding self-training for gradient-boosted trees. In *Advances in Neural Information Processing Systems (NeurIPS)*, volume 33, pp. 1651–1662, 2020.

Kwon, J. and Caramanis, C. The em algorithm gives sample-optimality for learning mixtures of well-separated gaussians. In *Conference on Learning Theory*, pp. 2425–2487. PMLR, 2020.

Laurent, B. and Massart, P. Adaptive estimation of a quadratic functional by model selection. *Annals of statistics*, pp. 1302–1338, 2000.

Lelarge, M. and Miolane, L. Asymptotic bayes risk for gaussian mixture in a semi-supervised setting. In *2019 IEEE 8th International Workshop on Computational Advances in Multi-Sensor Adaptive Processing (CAMSAP)*, pp. 639–643. IEEE, 2019.

Li, Y., Ildiz, M. E., Papailiopoulos, D., and Oymak, S. Transformers as algorithms: Generalization and stability in in-context learning. In *International Conference on Machine Learning*, pp. 19565–19594. PMLR, 2023.

Li, Y., Rawat, A. S., and Oymak, S. Fine-grained analysis of in-context linear estimation: Data, architecture, and beyond. *arXiv preprint arXiv:2407.10005*, 2024.

Mahankali, A. V., Hashimoto, T., and Ma, T. One step of gradient descent is provably the optimal in-context learner with one layer of linear self-attention. In *The Twelfth International Conference on Learning Representations*, 2024. URL https://openreview.net/forum?id=8p3fu56lKc.

Mignacco, F., Krzakala, F., Lu, Y., Urbani, P., and Zdeborova, L. The role of regularization in classification

of high-dimensional noisy gaussian mixture. In *International conference on machine learning*, pp. 6874–6883. PMLR, 2020.

Min, S., Lyu, X., Holtzman, A., Artetxe, M., Lewis, M., Hajishirzi, H., and Zettlemoyer, L. Rethinking the role of demonstrations: What makes in-context learning work? *arXiv preprint arXiv:2202.12837*, 2022.

Neopane, O. Lecture notes on high-dimensional statistics. https://www.stat.cmu.edu/~arinaldo/Teaching/36709/S19/Scribed_Lectures/Feb26_Ojash.pdf, 2018.

Nigam, K., McCallum, A. K., Thrun, S., and Mitchell, T. Text classification from labeled and unlabeled documents using em. *Machine Learning*, 39(2–3):103–134, 2000. doi: 10.1023/A:1007692713085.

Oymak, S. and Gulcu, T. C. Statistical and algorithmic insights for semi-supervised learning with self-training. *arXiv preprint arXiv:2006.11006*, 2020.

Qu, J., Holzmüller, D., Varoquaux, G., and Morvan, M. L. Tabicl: A tabular foundation model for in-context learning on large data. *arXiv preprint arXiv:2502.05564*, 2025.

Ratsaby, J. and Venkatesh, S. S. Learning from a mixture of labeled and unlabeled examples with parametric side information. In *Proceedings of the Eighth Annual Conference on Computational Learning Theory (COLT '95)*, pp. 412–417. ACM, 1995. doi: 10.1145/225298.225348.

Shen, W., Zhou, R., Yang, J., and Shen, C. On the training convergence of transformers for in-context classification. *arXiv preprint arXiv:2410.11778*, 2024.

Snell, C., Lee, J., Xu, K., and Kumar, A. Scaling llm test-time compute optimally can be more effective than scaling model parameters. *arXiv preprint arXiv:2408.03314*, 2024.

Thrampoulidis, C., Oymak, S., and Soltanolkotabi, M. Theoretical insights into multiclass classification: A high-dimensional asymptotic view. *Advances in Neural Information Processing Systems*, 33:8907–8920, 2020.

Von Oswald, J., Niklasson, E., Randazzo, E., Sacramento, J., Mordvintsev, A., Zhmoginov, A., and Vladymyrov, M. Transformers learn in-context by gradient descent. In *International Conference on Machine Learning*, pp. 35151–35174. PMLR, 2023.

Wang, K. and Thrampoulidis, C. Binary classification of gaussian mixtures: Abundance of support vectors, benign overfitting, and regularization. *SIAM Journal on Mathematics of Data Science*, 4(1):260–284, 2022.

Wang, Y., Wu, Y., Wei, Z., Jegelka, S., and Wang, Y. A theoretical understanding of self-correction through in-context alignment. In *The Thirty-eighth Annual Conference on Neural Information Processing Systems*.

Wei, C., Shen, K., Chen, Y., and Ma, T. Theoretical analysis of self-training with deep networks on unlabeled data. In *International Conference on Learning Representations (ICLR)*, 2021.

Wu, J., Zou, D., Chen, Z., Braverman, V., Gu, Q., and Bartlett, P. L. How many pretraining tasks are needed for in-context learning of linear regression? *arXiv preprint arXiv:2310.08391*, 2023.

Xie, S. M., Raghunathan, A., Liang, P., and Ma, T. An explanation of in-context learning as implicit bayesian inference. In *International Conference on Learning Representations*, 2022. URL https://openreview.net/forum?id=RdJVFCHjUMI.

Xu, J., Li, Z., Mukherjee, S., and Taylor, D. Towards understanding deep learning with persistent homology. *arXiv preprint arXiv:2106.06718*, 2021.

Zhang, R., Frei, S., and Bartlett, P. L. Trained transformers learn linear models in-context. *arXiv preprint arXiv:2306.09927*, 2023.

Zhang, R., Frei, S., and Bartlett, P. L. Trained transformers learn linear models in-context. *Journal of Machine Learning Research*, 25(49):1–55, 2024.

A. Related Work

Theoretical Analysis of In-Context Learning Recent work has developed theoretical frameworks for understanding in-context learning in transformers. Akyürek et al. (2023), Von Oswald et al. (2023) and Dai et al. (2023) demonstrated that transformers emulate gradient descent during ICL. Xie et al. (2022) offered a Bayesian perspective, while Zhang et al. (2023; 2024) showed transformers learn linear models in-context. Ahn et al. (2023) established they implement preconditioned gradient descent, and Mahankali et al. (2024) proved one-step gradient descent is optimal for single-layer linear attention. Works by Li et al. (2023) and Li et al. (2024) analyzed generalization capabilities of transformers. However, these frameworks exclusively focus on fully-supervised settings, leaving a critical gap in understanding how transformers handle partially labeled data—a common real-world scenario. Our work addresses this gap by providing the first theoretical characterization of semi-supervised in-context learning. (Wang et al.) considers a setting where the model observes demonstrations of the form (query, response$_i$, reward$_i$) and aims to correct its response based on the reward sequence. While our work has a different focus, it highlights that the model can correct/impute the missing labels in the context using implicit feedback from labeled demonstrations.

Semi-Supervised Learning Traditional semi-supervised learning (SSL) aims to leverage unlabeled data to improve classifier performance. For linear classifiers, Oymak & Gulcu (2020) characterized self-training iterations and demonstrated rejecting low-confidence samples; further theoretical analyses of self-training/pseudo-labeling cover deep networks (Wei et al., 2021) and models like gradient-boosted trees (Kumar et al., 2020). For Gaussian Mixture Models (GMMs), Lelarge & Miolane (2019) quantified maximal improvement from unlabeled data, while Krishnapuram et al. (2004) developed graph-based priors. Learning GMMs via Expectation-Maximization (EM) or pseudo-labeling, especially with few labels, is well-studied. Ratsaby & Venkatesh (1995) provided early PAC-style bounds for GMMs learned from few labeled and many unlabeled points. Balakrishnan et al. (2017) offered further statistical guarantees for EM. Nigam et al. (2000) demonstrated empirically that EM (viewable as iterative pseudo-labeling (Fan et al., 2023)) with pseudo-labels significantly reduces text classification error using unlabeled documents. These foundational works, with ongoing research in areas like agnostic learning (Kwon & Caramanis, 2020) and evolving theories (Xu et al., 2021), underpin many SSL concepts. While these works established fundamental principles, they did not consider how these concepts apply to in-context learning with transformers. Our contribution bridges this gap by showing how transformer depth enables effective utilization of unlabeled examples within the prompt, essentially implementing semi-supervised learning without parameter updates.

B. Experiments

In Sections 3 and 4, we introduced Figure 1 and demonstrated its consistency with our theoretical results. In this section, we describe the experimental setup and implementation details. Additionally, we present further empirical findings to investigate additional questions of interest. Motivated by Proposition 4.2, which suggests that looping can help leverage unlabeled data, Section B.2 introduces an algorithm based on the TabPFN, showing how it can enhance prediction performance by incorporating a small amount of unlabeled data and iterative pseudo-labeling through model looping.

Experimental Setup Following Section 2, set $d = 10$ and noise level $\sigma = 1$. All models are trained using Adam optimizer with a learning rate of 10^{-3} for 40,000 epochs, with a batch size of 512. We use logistic loss in our experiments. Since our study focuses on the optimization landscape and model expressivity, and experiments are implemented via gradient descent, we repeat 10 trainings from random initialization and results are presented as the maximal test accuracy among those 10 trails.

B.1. Additional Observations

• **Exploration of Optimal α Values.** In Section 4, we introduced the SSPI-k estimator (cf. (SSPI-k)), but did not discuss the choice of the mixing parameter α, which plays a crucial role in balancing the contribution of the supervised estimator $\hat{\boldsymbol{\mu}}_s$. Specifically, α controls how much weight is given to the purely supervised signal. In the fully supervised case, the optimal choice is $\alpha = 1$, as $\hat{\boldsymbol{\mu}}_s$ corresponds to the Bayes-optimal estimator.

In Figures 2(a) and 2(b), we empirically examine the optimal values of α. Given $\boldsymbol{\mu} \sim \text{Unif}(\mathbb{S}^{d-1})$, we define the optimal α as the minimizer of the following cosine similarity-based objective:

$$\alpha^\star := \min_{\alpha \in [0,1]} \mathcal{L}(\alpha) \quad \text{where} \quad \mathcal{L}(\alpha) = 1 - \mathbb{E}[\texttt{cosine\_similarity}(\boldsymbol{\mu}_{ss\text{-}k}, \boldsymbol{\mu})].$$

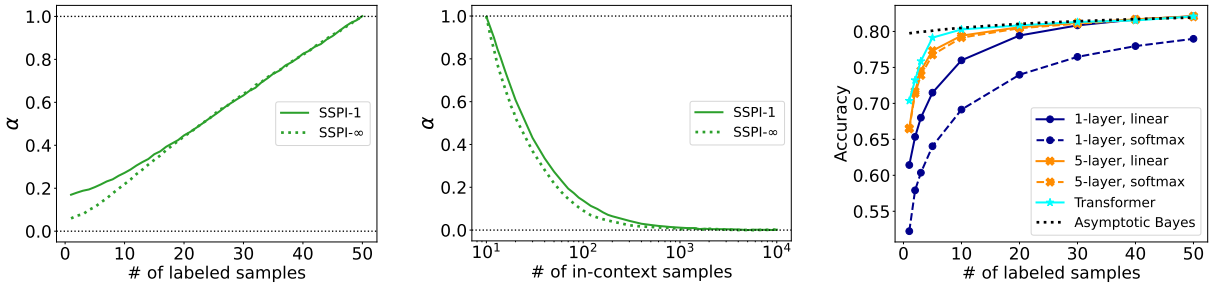

(a) $n = 50, p \in (0, 1]$. (b) $np = 10, n \in \{10, \cdots, 10000\}$. (c) $n = 50, p \in (0, 1]$.

Figure 2. Additional experimental results. (a)&(b): Analysis of the optimal α values for the SSPI estimator (cf. (SSPI-k)) under varying (n, p, k). Green solid and dotted curves represent optimal α values for SSPI-1 and SSPI-k, respectively. These experiments share the same settings as Figure1, and the SSPI results shown there use the corresponding α values from (a) and (b). (c): Comparison of different model architectures for the SS-ICL problem. Dark blue and orange curves show results for 1-layer and 5-layer attention models, with solid and dashed lines representing linear and softmax attention, respectively. Cyan curves correspond to 5-layer Transformers. The black dotted line shows the asymptotic Bayes-optimal error (cf. (Lelarge & Miolane, 2019)). Results suggest the performance ordering: Transformer $>$ linear attention $>$ softmax attention. Further details are provided in Section B.

For each setting, we optimize α using the Adam optimizer for 10,000 epochs with a batch size of 128 and a learning rate of 0.01. The results are shown in Figs 2(a) and 2(b).

In Figure 2(a), for both SSPI-1 and SSPI-∞, the optimal α starts near zero when the number of labeled examples is small, reflecting the limited utility of $\hat{\boldsymbol{\mu}}_s$ in low-supervision regimes. As the number of labeled samples increases, α grows approximately linearly and approaches 1 when the problem becomes fully supervised. In Figure 2(b), when $n = 10$ and $p = 1$ (i.e., all examples are labeled), the optimal α begins at 1. As n increases and the fraction of unlabeled data grows, α decreases significantly. This trend indicates that as the volume of unlabeled data increases, the SSPI estimator adaptively reduces reliance on the supervised component $\hat{\boldsymbol{\mu}}_s$ and increases reliance on the semi-supervised component, which leverages the structure of the unlabeled data through $\boldsymbol{X}^\top \boldsymbol{X}$.

• **Comparison Across Different Model Architectures.** Beyond linear attention, we investigate additional model architectures under our SS-ICL setting. The comparison results are presented in Fig. 2(c). The softmax attention model uses the same structure described in Section 2.2, with the only difference being the addition of a softmax operation in Eq. (3). The Transformer model introduces further nonlinearity and capacity by incorporating multi-layer perceptrons (MLPs) and layer normalization. The Transformer experiments are conducted with 5-layer models.

When comparing weaker models—such as 1-layer linear (dark blue solid) and softmax (dark blue dashed) attention—we observe that softmax attention consistently underperforms linear attention. Notably, softmax attention fails to match the performance of the optimal supervised estimator, even when all labels are observed (i.e., when the number of labeled samples equals $n = 50$). Furthermore, increasing the depth of softmax attention (orange dashed curve for 5-layer softmax) still does not surpass the performance of 5-layer linear attention (orange solid curve). Among all architectures, the Transformer achieves the best performance due to its increased model capacity and expressiveness. Compared with Fig. 1(a), where the orange and dark blue markers (linear attention) are identical, the Transformer significantly improves accuracy. This improvement highlights that SSPI, while effective, is not the optimal semi-supervised estimator. Although our semi-supervised setting assumes isotropic data, the characterization of its optimal algorithm remains an open and foundational problem for future exploration. In the figure, we also include the asymptotic Bayes-optimal curve (black dotted; derived from (Lelarge & Miolane, 2019)) . As the number of samples increases, the results from linear attention, softmax attention, and Transformer all converge toward this optimal curve. We attribute the initial performance gap, particularly at low values of np (e.g., $np = 1$), to the scarcity of labeled data.

B.2. Tabular Experiments

To further investigate how model looping (Proposition 4.2) can improve label prediction, we introduce an algorithm that addresses unlabeled data by iteratively assigning pseudo-labels. We evaluate the algorithm on real-world datasets, with results presented in Table 1. We evaluated the effectiveness of our proposed looping strategy by iteratively applying

Table 1. Testing accuracy comparison between the baseline (trained on labeled samples only) and after 1 or 5 iterations of looping TabPFN-v2. Results are averaged over 20 random training.

Dataset	OpenML1049		OpenML1464		OpenML1067		OpenML1494		OpenML1489		OpenML40981	
	10/10	20/20	10/10	20/20	10/10	20/20	10/10	20/20	10/10	20/20	10/10	20/20
Baseline	0.7497	0.8495	0.5707	0.7172	0.6883	0.7700	0.5914	0.6973	0.6216	0.6775	0.7420	0.7396
Loop-1	0.7929	0.8476	0.6066	0.7333	0.7160	0.8084	0.6091	0.6965	0.6555	0.7138	0.7445	0.7719
Loop-5	0.8287	0.8421	0.7178	0.7243	0.7710	0.8109	0.6394	0.7016	0.7016	0.7158	0.7578	0.7761

TabPFN-v2 on real-world binary classification benchmarks from (Hollmann et al., 2025). We tested two settings with equal numbers of labeled and unlabeled samples: (10, 10) and (20, 20). In each experiment, we first use the labeled data to assign soft pseudo-labels to the unlabeled data based on TabPFN-v2 predictions. These pseudo-labels are then updated iteratively through repeated looping, and each loop, we feed the model with both labeled and pseudo-labeled data. Full implementation details are provided in the supplementary material.

The results are summarized in Table 1, and each is averaged over 20 random training and test data splits. As a baseline, we use TabPFN-v2 feeding with only the labeled data to make one-shot predictions on the test set. We compare this to models after 1 iteration (Loop-1) and 5 iterations (Loop-5) of pseudo-label refinement. Our results show that the looping strategy significantly improves test accuracy. For instance, on the OpenML1464 dataset with 10 unlabeled examples, Loop-5 improves the baseline accuracy by approximately 25.8%. Notably, in some cases—such as OpenML1489—the (10 labeled, 10 unlabeled) setup with 5 loops outperforms the (20 labeled, 0 unlabeled) baseline, demonstrating the effectiveness of leveraging unlabeled data. These findings highlight that explicitly looping the tabular foundation model to iteratively refine soft pseudo-labels can substantially enhance performance by effectively incorporating information from unlabeled data.

C. Discussion and Limitations

Our paper introduces a theoretical study of semisupervised in-context learning and characterizes how transformer, specifically linear attention, models can harness unlabeled data in their context window to make inference. We show that depth is crucial to go beyond supervised estimation and utilize unlabeled data, and the latter is achieved by constructing estimators of the form $\hat{\boldsymbol{\mu}} = \sum_{i\geq 0}^{K} a_i (\boldsymbol{X}^\top \boldsymbol{X})^i \boldsymbol{X}^\top \boldsymbol{y}$. $\log K$ depth suffices to express a Kth order polynomial which is in line with our synthetic and real experiments that corroborate that mild amount of depth/looping already achieves most of the benefit. Our core theoretical results are limited to linear attention models and it is important to understand the capabilities of the full transformer architecture. Indeed, transformer (MLP+softmax) empirically outperforms a linear attention model with equal number of layers, well approximating the Bayes optimal semisupervised estimator. It would also be exciting to go beyond the classification setting and examine how self-generated CoT rationales, as in (Wu et al., 2023), can enhance ICL capabilities for tasks that require reasoning/autoregression.

D. Analysis of Single-layer Linear Attention

D.1. Supporting Lemmas

Recap the SPI estimator from (SPI). Given a semi-supervised dataset $(\boldsymbol{x}_i, y_i)_{i=1}^n$ as described in Section 2.1, let $\mathcal{I}$ denote the token indices set corresponding to the labeled demonstrations, that is, we have

$$y_i = \begin{cases} y_i^c, & i \in \mathcal{I} \\ 0, & otherwise. \end{cases} \tag{12}$$

Then, the SPI estimates the task mean via

$$\hat{\boldsymbol{\mu}}_s = \frac{1}{|\mathcal{I}|} \sum_{i\in\mathcal{I}} y_i \boldsymbol{x}_i.$$

Let $\boldsymbol{W} \in \mathbb{R}^{d\times d}$ be the preconditioning matrix. We define the following objective:

$$\boldsymbol{W}^\star := \arg\min_{\boldsymbol{W}\in\mathbb{R}^{d\times d}} \tilde{\mathcal{L}}(\boldsymbol{W}) \quad \text{where} \quad \tilde{\mathcal{L}}(\boldsymbol{W}) = \mathbb{E}\left[\left(\boldsymbol{x}^\top \boldsymbol{W} \sum_{i\in\mathcal{I}} y_i \boldsymbol{x}_i - y\right)^2\right]. \tag{13}$$

Here, we set $(\boldsymbol{x}, y)$ to be the query feature and its corresponding true label. The expectation subsumes the randomness in $(\boldsymbol{x}_i, y_i), (\boldsymbol{x}, y)$ as described in Section 2.1.

In this section, we provide a lemma that establishes equivalence between optimizing $\mathcal{L}_{\text{att-1}}(\mathcal{W}, \boldsymbol{h})$ (cf. (5) and choosing $L = 1$) and $\tilde{\mathcal{L}}(\boldsymbol{W})$.

Lemma D.1. *Consider ICL problem described in Section 2.2 with prompt defined in (2). Consider training with a single-layer linear attention with squared loss, that is, $L = 1$ and $\ell(y, \hat{y}) = (y - \hat{y})^2$. Recall the objectives from (5) and (13), and let $\mathcal{L}^\star_{\text{att-1}}$ and $\tilde{\mathcal{L}}^\star := \tilde{\mathcal{L}}(\boldsymbol{W}^\star)$ be their corresponding optimal losses. Then, we have*

$$\mathcal{L}^\star_{\text{att-1}} = \tilde{\mathcal{L}}^\star. \tag{14}$$

Additionally, let $f^\star_{\text{att-1}} : \mathbb{R}^{(n+1)\times(d+1)} \to \mathbb{R}$ denote the optimal prediction (associated with the optimal loss $\mathcal{L}^\star_{\text{att-1}}$). We have that $f^\star_{\text{att-1}}$ is unique and for any prompt $\boldsymbol{Z}$ (cf. (2))

$$f^\star_{\text{att-1}}(\boldsymbol{Z}) = \boldsymbol{x}^\top \boldsymbol{W}^\star \sum_{i \in \mathcal{I}} y_i \boldsymbol{x}_i. \tag{15}$$

Proof. Recap the single-layer linear attention model and its prediction from (3) and (4). We have

$$f_{\text{att-1}}(\boldsymbol{Z}) = \boldsymbol{h}^\top \text{att}(\boldsymbol{Z}; \mathcal{W})_{[n+1]} \quad \text{where} \quad \text{att}(\boldsymbol{Z}; \mathcal{W}) = (\boldsymbol{Z}\boldsymbol{W}_q \boldsymbol{W}_k^\top \boldsymbol{Z}^\top) \boldsymbol{M} \boldsymbol{Z} \boldsymbol{W}_v \tag{16}$$

with $\mathcal{W} := \{\boldsymbol{W}_q, \boldsymbol{W}_k, \boldsymbol{W}_v\}$ being the set of the query, key and value matrices of the attention. Since $\mathcal{W}$ and $\boldsymbol{h}$ are tunable parameters, without loss of generality and for simplicity, let

$$\boldsymbol{W} := \boldsymbol{W}_q \boldsymbol{W}_k^\top \quad \text{and} \quad \bar{\boldsymbol{h}} := \boldsymbol{W}_v \boldsymbol{h}.$$

Following the proof of Li et al., 2024, Proposition 1, similarly, we denote

$$\boldsymbol{W} = \begin{bmatrix} \bar{\boldsymbol{W}} & \boldsymbol{w}_1 \\ \boldsymbol{w}_2^\top & w \end{bmatrix} \qquad \text{and} \qquad \bar{\boldsymbol{h}} = \begin{bmatrix} \boldsymbol{h}_1 \\ h \end{bmatrix},$$

where $\bar{\boldsymbol{W}} \in \mathbb{R}^{d\times d}$, $\boldsymbol{w}_1, \boldsymbol{w}_2, \boldsymbol{h}_1 \in \mathbb{R}^d$, and $w, h \in \mathbb{R}$.

Additionally, let $\mathcal{I}$ denote the token indices set corresponding to the labeled demonstrations (cf. 12). Recall the prompt $\boldsymbol{Z}$ from (2), and $\boldsymbol{X} = [\boldsymbol{x}_1 \ \cdots \ \boldsymbol{x}_n]^\top \in \mathbb{R}^{n\times d}$ and $\boldsymbol{y} = [y_1 \ \cdots \ y_n]^\top \in \mathbb{R}^n$ from (8). Then we get

$$\boldsymbol{Z} = \begin{bmatrix} \boldsymbol{x}_1 & \boldsymbol{x}_2 & \cdots & \boldsymbol{x}_n & \boldsymbol{x} \\ y_1 & y_2 & \cdots & y_n & 0 \end{bmatrix}^\top = \begin{bmatrix} \boldsymbol{X}^\top & \boldsymbol{x} \\ \boldsymbol{y}^\top & 0 \end{bmatrix}^\top \in \mathbb{R}^{(n+1)\times(d+1)}. \tag{17}$$

Combining (16) and (17) together, we can rewrite the one-layer linear prediction as

$$\begin{aligned}
f_{\text{att-1}}(\boldsymbol{Z}) &= [\boldsymbol{x}^\top \ 0] \boldsymbol{W} \boldsymbol{Z}^\top \boldsymbol{M} \boldsymbol{Z} \bar{\boldsymbol{h}} \\
&= [\boldsymbol{x}^\top \ 0] \begin{bmatrix} \bar{\boldsymbol{W}} & \boldsymbol{w}_1 \\ \boldsymbol{w}_2^\top & w \end{bmatrix} \begin{bmatrix} \boldsymbol{X}^\top & \boldsymbol{x} \\ \boldsymbol{y}^\top & 0 \end{bmatrix} \begin{bmatrix} \boldsymbol{I}_n & 0 \\ 0 & 0 \end{bmatrix} \begin{bmatrix} \boldsymbol{X}^\top & \boldsymbol{x} \\ \boldsymbol{y}^\top & 0 \end{bmatrix}^\top \begin{bmatrix} \boldsymbol{h}_1 \\ h \end{bmatrix} \\
&= [\boldsymbol{x}^\top \bar{\boldsymbol{W}} \ \ \boldsymbol{x}^\top \boldsymbol{w}_1] \begin{bmatrix} \boldsymbol{X}^\top \boldsymbol{X} & \boldsymbol{X}^\top \boldsymbol{y} \\ \boldsymbol{y}^\top \boldsymbol{X} & \boldsymbol{y}^\top \boldsymbol{y} \end{bmatrix} \begin{bmatrix} \boldsymbol{h}_1 \\ h \end{bmatrix} \\
&= [\boldsymbol{x}^\top \bar{\boldsymbol{W}} \ \ \boldsymbol{x}^\top \boldsymbol{w}_1] \begin{bmatrix} \boldsymbol{X}^\top \boldsymbol{X} \boldsymbol{h}_1 + h \boldsymbol{X}^\top \boldsymbol{y} \\ \boldsymbol{y}^\top \boldsymbol{X} \boldsymbol{h}_1 + h \boldsymbol{y}^\top \boldsymbol{y} \end{bmatrix} \\
&= \boldsymbol{x}^\top \bar{\boldsymbol{W}} (\boldsymbol{X}^\top \boldsymbol{X} \boldsymbol{h}_1 + h \boldsymbol{X}^\top \boldsymbol{y}) + \boldsymbol{x}^\top \boldsymbol{w}_1 (\boldsymbol{y}^\top \boldsymbol{X} \boldsymbol{h}_1 + h \boldsymbol{y}^\top \boldsymbol{y}) \\
&= \boldsymbol{x}^\top (h \bar{\boldsymbol{W}} + \boldsymbol{w}_1 \boldsymbol{h}_1^\top) \boldsymbol{X}^\top \boldsymbol{y} + \boldsymbol{x}^\top (\bar{\boldsymbol{W}} \boldsymbol{X}^\top \boldsymbol{X} \boldsymbol{h}_1 + h \boldsymbol{y}^\top \boldsymbol{y} \boldsymbol{w}_1) \\
&= \boldsymbol{x}^\top \tilde{\boldsymbol{W}} \boldsymbol{X}^\top \boldsymbol{y} + \boldsymbol{x}^\top (\bar{\boldsymbol{W}} \boldsymbol{X}^\top \boldsymbol{X} \boldsymbol{h}_1 + m h \boldsymbol{w}_1)
\end{aligned}$$

where $\tilde{\boldsymbol{W}} := h \bar{\boldsymbol{W}} + \boldsymbol{w}_1 \boldsymbol{h}_1^\top$ and we define $m := |\mathcal{I}|$.

Next, recall the loss from (5) and consider the squared loss function, $\ell(y, \hat{y}) = (y - \hat{y})^2$. We have

$$\begin{aligned}
\mathcal{L}_{\text{att-1}}(\mathcal{W}, \boldsymbol{h}) &= \mathbb{E}\left[(f_{\text{att-1}}(\boldsymbol{Z}) - y)^2\right] \\
&= \mathbb{E}\left[\left(\boldsymbol{x}^\top \tilde{\boldsymbol{W}} \boldsymbol{X}\boldsymbol{y} + \boldsymbol{x}^\top \left(\bar{\boldsymbol{W}} \boldsymbol{X}^\top \boldsymbol{X} \boldsymbol{h}_1 + mh\boldsymbol{w}_1\right) - y\right)^2\right] \\
&= \mathbb{E}\left[\left(y\boldsymbol{x}^\top \tilde{\boldsymbol{W}} \boldsymbol{X}\boldsymbol{y} + y\boldsymbol{x}^\top \left(\bar{\boldsymbol{W}} \boldsymbol{X}^\top \boldsymbol{X} \boldsymbol{h}_1 + mh\boldsymbol{w}_1\right) - 1\right)^2\right].
\end{aligned}$$

For simplicity and without loss of generality, we omit y and use $\boldsymbol{x}$ to represent $y\boldsymbol{x}$. Note that the distribution of (updated) $\boldsymbol{x}$ is not conditioned on its class and given mean vector $\boldsymbol{\mu}$, it follows $\boldsymbol{x} \sim \mathcal{N}(\boldsymbol{\mu}, \sigma^2 \boldsymbol{I})$. Similarly, let $\boldsymbol{x}_i$ represent $y_i^c \boldsymbol{x}_i$. We can then write

$$\begin{aligned}
\mathcal{L}_{\text{att-1}}(\mathcal{W}, \boldsymbol{h}) &= \mathbb{E}\left[\left(\boldsymbol{x}^\top \tilde{\boldsymbol{W}} \sum_{i \in \mathcal{I}} \boldsymbol{x}_i + \boldsymbol{x}^\top \left(\bar{\boldsymbol{W}} \boldsymbol{X}^\top \boldsymbol{X} \boldsymbol{h}_1 + mh\boldsymbol{w}_1\right) - 1\right)^2\right] \\
&= \mathbb{E}\left[\left(\boldsymbol{x}^\top \tilde{\boldsymbol{W}} \sum_{i \in \mathcal{I}} \boldsymbol{x}_i - 1\right)^2\right] + \mathbb{E}\left[\left(\boldsymbol{x}^\top \left(\bar{\boldsymbol{W}} \boldsymbol{X}^\top \boldsymbol{X} \boldsymbol{h}_1 + mh\boldsymbol{w}_1\right)\right)^2\right] \\
&\quad + 2\,\mathbb{E}\left[\left(\boldsymbol{x}^\top \tilde{\boldsymbol{W}} \sum_{i \in \mathcal{I}} \boldsymbol{x}_i - 1\right)\left(\boldsymbol{x}^\top \left(\bar{\boldsymbol{W}} \boldsymbol{X}^\top \boldsymbol{X} \boldsymbol{h}_1 + mh\boldsymbol{w}_1\right)\right)\right].
\end{aligned} \tag{18}$$

We start with showing that for any given parameters $\boldsymbol{W} \in \mathbb{R}^{(d+1)\times(d+1)}, \boldsymbol{h} \in \mathbb{R}^{d+1}$, $\mathbb{E}\left[\left(\boldsymbol{x}^\top \tilde{\boldsymbol{W}} \sum_{i \in \mathcal{I}} \boldsymbol{x}_i - 1\right)\left(\boldsymbol{x}^\top \left(\bar{\boldsymbol{W}} \boldsymbol{X}^\top \boldsymbol{X} \boldsymbol{h}_1 + mh\boldsymbol{w}_1\right)\right)\right] = 0$. To prove it, we first expand

$$\begin{aligned}
&(\boldsymbol{x}^\top \tilde{\boldsymbol{W}} \sum_{i \in \mathcal{I}} \boldsymbol{x}_i - 1)(\boldsymbol{x}^\top (\bar{\boldsymbol{W}} \boldsymbol{X}^\top \boldsymbol{X} \boldsymbol{h}_1 + mh\boldsymbol{w}_1)) \\
&= \underbrace{(\boldsymbol{x}^\top \tilde{\boldsymbol{W}} \sum_{i \in \mathcal{I}} \boldsymbol{x}_i)(\boldsymbol{x}^\top \bar{\boldsymbol{W}} \boldsymbol{X}^\top \boldsymbol{X} \boldsymbol{h}_1)}_{(a)} - \underbrace{\boldsymbol{x}^\top \bar{\boldsymbol{W}} \boldsymbol{X}^\top \boldsymbol{X} \boldsymbol{h}_1}_{(b)} + \underbrace{(\boldsymbol{x}^\top \tilde{\boldsymbol{W}} \sum_{i \in \mathcal{I}} \boldsymbol{x}_i)(mh\boldsymbol{x}^\top \boldsymbol{w}_1)}_{(c)} - \underbrace{mh\boldsymbol{x}^\top \boldsymbol{w}_1}_{(d)}.
\end{aligned}$$

In the following, we consider the expectations of $(a), (b), (c), (d)$ sequentially, all of which take the value zero. First note that since $\boldsymbol{\mu} \sim \text{Unif}(\mathbb{S}^{d-1})$ and $(\boldsymbol{\xi}_i)_{i=1}^n, \boldsymbol{\xi} \sim \mathcal{N}(0, \sigma^2 \boldsymbol{I})$, the odd moments of $\boldsymbol{\mu}$, $\boldsymbol{\xi}$ and $\boldsymbol{\xi}_i, i \in [n]$ are all zeros.

$$\begin{aligned}
(a): \quad & \mathbb{E}\left[(\boldsymbol{x}^\top \tilde{\boldsymbol{W}} \sum_{i \in \mathcal{I}} \boldsymbol{x}_i)(\boldsymbol{x}^\top \bar{\boldsymbol{W}} \boldsymbol{X}^\top \boldsymbol{X} \boldsymbol{h}_1)\right] \\
&= \mathbb{E}\left[(\boldsymbol{\mu} + \boldsymbol{\xi})^\top \tilde{\boldsymbol{W}} \sum_{i \in \mathcal{I}} (\boldsymbol{\mu} + \boldsymbol{\xi}_i)(\boldsymbol{\mu} + \boldsymbol{\xi})^\top \bar{\boldsymbol{W}} \sum_{i \in [n]} (\boldsymbol{\mu} + \boldsymbol{\xi}_i)(\boldsymbol{\mu} + \boldsymbol{\xi}_i)^\top \boldsymbol{h}_1\right] \\
&= \sum_{i \in \mathcal{I}} \sum_{j \in [n]} \mathbb{E}\left[(\boldsymbol{\mu} + \boldsymbol{\xi})^\top \tilde{\boldsymbol{W}} (\boldsymbol{\mu} + \boldsymbol{\xi}_i)(\boldsymbol{\mu} + \boldsymbol{\xi})^\top \bar{\boldsymbol{W}} (\boldsymbol{\mu} + \boldsymbol{\xi}_j)(\boldsymbol{\mu} + \boldsymbol{\xi}_j)^\top \boldsymbol{h}_1\right] \\
&= \sum_{i \in \mathcal{I}} \sum_{j \in [n]} \mathbb{E}\left[\boldsymbol{\mu}^\top \tilde{\boldsymbol{W}} \boldsymbol{\mu}\boldsymbol{\mu}^\top \bar{\boldsymbol{W}} (\boldsymbol{\mu}\boldsymbol{\mu}^\top + \boldsymbol{\xi}_j \boldsymbol{\xi}_j^\top) \boldsymbol{h}_1 + \boldsymbol{\xi}^\top \tilde{\boldsymbol{W}} \boldsymbol{\mu} \boldsymbol{\xi}^\top \bar{\boldsymbol{W}} (\boldsymbol{\mu}\boldsymbol{\mu}^\top + \boldsymbol{\xi}_j \boldsymbol{\xi}_j^\top) \boldsymbol{h}_1\right] \\
&= 0,
\end{aligned}$$

$$
\begin{aligned}
(b): \quad & \mathbb{E}\left[\boldsymbol{x}^\top \bar{\boldsymbol{W}} \boldsymbol{X}^\top \boldsymbol{X} \boldsymbol{h}_1\right] \\
& = \mathbb{E}\left[(\boldsymbol{\mu}+\boldsymbol{\xi})^\top \bar{\boldsymbol{W}} \sum_{i\in[n]} (\boldsymbol{\mu}+\boldsymbol{\xi}_i)(\boldsymbol{\mu}+\boldsymbol{\xi}_i)^\top \boldsymbol{h}_1\right] \\
& = \mathbb{E}\left[\boldsymbol{\mu}^\top \bar{\boldsymbol{W}} \sum_{i\in[n]} (\boldsymbol{\mu}\boldsymbol{\mu}^\top + \boldsymbol{\xi}_i\boldsymbol{\xi}_i^\top) \boldsymbol{h}_1\right] \\
& = 0,
\end{aligned}
$$

$$
\begin{aligned}
(c): \quad & \mathbb{E}\left[(\boldsymbol{x}^\top \tilde{\boldsymbol{W}} \sum_{i\in\mathcal{I}} \boldsymbol{x}_i)(mh\boldsymbol{x}^\top \boldsymbol{w}_1)\right] \\
& = mh\,\mathbb{E}\left[(\boldsymbol{\mu}+\boldsymbol{\xi})^\top \tilde{\boldsymbol{W}} \sum_{i\in\mathcal{I}} (\boldsymbol{\mu}+\boldsymbol{\xi}_i)(\boldsymbol{\mu}+\boldsymbol{\xi})^\top \boldsymbol{w}_1\right] \\
& = mh \sum_{i\in\mathcal{I}} \mathbb{E}\left[(\boldsymbol{\mu}+\boldsymbol{\xi})^\top \tilde{\boldsymbol{W}} \boldsymbol{\mu} (\boldsymbol{\mu}+\boldsymbol{\xi})^\top \boldsymbol{w}_1\right] \\
& = mh \sum_{i\in\mathcal{I}} \mathbb{E}\left[\boldsymbol{\mu}^\top \tilde{\boldsymbol{W}} \boldsymbol{\mu}\boldsymbol{\mu}^\top \boldsymbol{w}_1 + \boldsymbol{\xi}^\top \tilde{\boldsymbol{W}} \boldsymbol{\mu}\boldsymbol{\xi}^\top \boldsymbol{w}_1\right] \\
& = 0,
\end{aligned}
$$

$$
(d): \quad \mathbb{E}\left[mh\boldsymbol{x}^\top \boldsymbol{w}_1\right] = 0.
$$

Therefore, loss in (18) returns

$$
\mathcal{L}_{\text{att-1}}(\mathcal{W}, \boldsymbol{h}) = \underbrace{\mathbb{E}\left[\left(\boldsymbol{x}^\top \tilde{\boldsymbol{W}} \sum_{i\in\mathcal{I}} \boldsymbol{x}_i - 1\right)^2\right]}_{\tilde{\mathcal{L}}(\tilde{\boldsymbol{W}})} + \mathbb{E}\left[\left(\boldsymbol{x}^\top (\bar{\boldsymbol{W}} \boldsymbol{X}^\top \boldsymbol{X} \boldsymbol{h}_1 + mh\boldsymbol{w}_1)\right)^2\right].
$$

Here, the first term $\mathbb{E}[(\boldsymbol{x}^\top \tilde{\boldsymbol{W}} \sum_{i\in\mathcal{I}} \boldsymbol{x}_i - 1)^2] = \tilde{\mathcal{L}}(\tilde{\boldsymbol{W}})$ where $\tilde{\mathcal{L}}(\tilde{\boldsymbol{W}})$ is defined in (13).

Recall that $\tilde{\boldsymbol{W}} = h\bar{\boldsymbol{W}} + \boldsymbol{w}_1\boldsymbol{h}_1^\top$. Then for any $\tilde{\boldsymbol{W}} \in \mathbb{R}^{d\times d}$, setting $\boldsymbol{h}_1 = \boldsymbol{w}_1 = \boldsymbol{0}_d$ and $h = 1$ returns $\mathbb{E}\left[\left(\boldsymbol{x}^\top \left(\bar{\boldsymbol{W}} \boldsymbol{X}^\top \boldsymbol{X} \boldsymbol{h}_1 + mh\boldsymbol{w}_1\right)\right)^2\right] = 0$, and then

$$
\mathcal{L}_{\text{att-1}}(\mathcal{W}, \boldsymbol{h}) = \mathbb{E}\left[\left(\boldsymbol{x}^\top \bar{\boldsymbol{W}} \sum_{i\in\mathcal{I}} \boldsymbol{x}_i - 1\right)^2\right]
$$

Therefore, optimizing $\mathcal{L}_{\text{att-1}}(\mathcal{W}, \boldsymbol{h})$ returns the same minima as optimizing $\tilde{\mathcal{L}}(\boldsymbol{W})$, which completes the proof of (14). Note that optimal loss $\mathcal{L}^\star_{\text{att-1}}$ depends on the labeled data $i \in \mathcal{I}$ only.

Furthermore, since $\tilde{\mathcal{L}}(\boldsymbol{W})$ is strongly convex (see (19)), $\boldsymbol{W}^\star$ exists and is unique. Therefore, (14) and uniqueness of $\boldsymbol{W}^\star$ leads to the conclusion (15). □

Lemma D.2. *Consider the objective defined in* (13) *with semi-supervised data following Section 2. Then the optimal solution* $\boldsymbol{W}^\star$ *satisfies*

$$
\boldsymbol{W}^\star = c\boldsymbol{I}
$$

for some $c > 0$.

Proof. Recap the Objective (13) and its optimal solution $\boldsymbol{W}^\star$. Let $\mathcal{I}$ be the index set corresponding the labeled in-context examples, and $|\mathcal{I}| = m$. Note that, m is also a random variable, independent of $\boldsymbol{x}_i, y_i^c, \boldsymbol{x}, y$.

As in the proof of Lemma D.1, we use $\boldsymbol{x}$ to represent $y\boldsymbol{x}$ and $\boldsymbol{x}_i$ to represent $y_i^c \boldsymbol{x}_i$ for simplicity, where (updated) $\boldsymbol{x}_i, \boldsymbol{x} \sim \mathcal{N}(\boldsymbol{\mu}, \sigma^2 \boldsymbol{I})$. Letting $\boldsymbol{\xi}', \boldsymbol{\xi}, \boldsymbol{\xi}_i \sim \mathcal{N}(0, \sigma^2 \boldsymbol{I})$ be independent, we obtain

$$
\begin{aligned}
\tilde{\mathcal{L}}(\boldsymbol{W}) &= \mathbb{E}\left[(\boldsymbol{x}^\top \boldsymbol{W} \sum_{i \in \mathcal{I}} \boldsymbol{x}_i - 1)^2\right] \\
&= \mathbb{E}\left[((\boldsymbol{\mu} + \boldsymbol{\xi})^\top \boldsymbol{W} \sum_{i \in \mathcal{I}} (\boldsymbol{\mu} + \boldsymbol{\xi}_i) - 1)^2\right] \\
&= \mathbb{E}\left[((\boldsymbol{\mu} + \boldsymbol{\xi})^\top \boldsymbol{W} (m\boldsymbol{\mu} + \sqrt{m}\boldsymbol{\xi}') - 1)^2\right] \\
&= \mathbb{E}\left[m^2 (\boldsymbol{\mu}^\top \boldsymbol{W} \boldsymbol{\mu})^2 + m(\boldsymbol{\mu}^\top \boldsymbol{W} \boldsymbol{\xi}')^2 + m^2 (\boldsymbol{\xi}^\top \boldsymbol{W} \boldsymbol{\mu})^2 + m(\boldsymbol{\xi}^\top \boldsymbol{W} \boldsymbol{\xi}')^2 + 1\right] - 2\,\mathbb{E}\left[m \boldsymbol{\mu}^\top \boldsymbol{W} \boldsymbol{\mu}\right] \\
&= \frac{\mathbb{E}[m^2]}{d(d+2)} (\mathtt{tr}(\boldsymbol{W})^2 + \mathtt{tr}(\boldsymbol{W}\boldsymbol{W}^\top) + \mathtt{tr}(\boldsymbol{W}^2)) + \frac{\mathbb{E}[m + m^2]}{d} \sigma^2 \mathtt{tr}(\boldsymbol{W}\boldsymbol{W}^\top) \\
&\quad + \mathbb{E}[m] \sigma^4 \mathtt{tr}(\boldsymbol{W}\boldsymbol{W}^\top) + 1 - \frac{2\,\mathbb{E}[m]}{d} \mathtt{tr}(\boldsymbol{W}).
\end{aligned} \tag{19}
$$

Differentiating it results in

$$
\nabla_{\boldsymbol{W}} \tilde{\mathcal{L}}(\boldsymbol{W}) = \frac{2\,\mathbb{E}[m^2]}{d(d+2)} (\mathtt{tr}(\boldsymbol{W})\boldsymbol{I} + \boldsymbol{W} + \boldsymbol{W}^\top) + \frac{2\,\mathbb{E}[m + m^2]\sigma^2}{d} \boldsymbol{W} + 2\,\mathbb{E}[m]\sigma^4 \boldsymbol{W} - \frac{2\,\mathbb{E}[m]}{d} \boldsymbol{I}.
$$

Setting $\nabla_{\boldsymbol{W}} \tilde{\mathcal{L}}(\boldsymbol{W}) = 0$, we obtain the unique optimal $\boldsymbol{W}^\star$

$$
\boldsymbol{W}^\star = \frac{1}{(1+\sigma^2)\,\mathbb{E}[m^2]/\,\mathbb{E}[m] + \sigma^2 + \sigma^4 d} \boldsymbol{I},
$$

which leads to the conclusion that $\boldsymbol{W}^\star = c\boldsymbol{I}$, for $c = \frac{1}{(1+\sigma^2)\,\mathbb{E}[m^2]/\,\mathbb{E}[m] + \sigma^2 + \sigma^4 d} > 0$. It completes the proof. □

D.2. Proof of Theorem 3.1

Proof. Note that (6) can be easily proven using Lemmas D.1 and D.2. Then, we focus on proving (7).

Given that (6) holds, we can rewrite its classification error as

$$
\mathbb{P}(y^\star_{\text{att-1}}(\boldsymbol{Z}) \neq y) = \mathbb{P}(\mathrm{sgn}(\boldsymbol{x}^\top \hat{\boldsymbol{\mu}}_s) \neq y) = \mathbb{P}(\mathrm{sgn}(y\boldsymbol{x}^\top \hat{\boldsymbol{\mu}}_s) \neq 1) \tag{20}
$$

where $\hat{\boldsymbol{\mu}}_s = \frac{1}{|\mathcal{I}|} \sum_{i \in \mathcal{I}} y_i \boldsymbol{x}_i$ defined in (SPI) and $\mathcal{I}$ is the index set of labeled samples. Let $m = |\mathcal{I}|$.

Recall from Section 2.1 where $\boldsymbol{x} \sim \mathcal{N}(y \cdot \boldsymbol{\mu}, \sigma^2 \boldsymbol{I})$. We can rewrite

$$
y\boldsymbol{x} = \boldsymbol{\mu} + \sigma \boldsymbol{g}_1 \quad \text{where} \quad \boldsymbol{g}_1 \sim \mathcal{N}(0, \boldsymbol{I}).
$$

Then for any given $\boldsymbol{\mu}, \hat{\boldsymbol{\mu}}_s$, we get

$$
\begin{aligned}
\mathbb{P}\left(\mathrm{sgn}(y\boldsymbol{x}^\top \hat{\boldsymbol{\mu}}_s) \neq 1 \,\middle|\, \boldsymbol{\mu}, \hat{\boldsymbol{\mu}}_s\right) &= \mathbb{P}\left((\boldsymbol{\mu} + \sigma \boldsymbol{g}_1)^\top \hat{\boldsymbol{\mu}}_s < 0 \,\middle|\, \boldsymbol{\mu}, \hat{\boldsymbol{\mu}}_s\right) \\
&= \mathbb{P}\left(\boldsymbol{\mu}^\top \hat{\boldsymbol{\mu}}_s < \sigma \boldsymbol{g}_1^\top \hat{\boldsymbol{\mu}}_s \,\middle|\, \boldsymbol{\mu}, \hat{\boldsymbol{\mu}}_s\right) \\
&= Q\left(\frac{\boldsymbol{\mu}^\top \hat{\boldsymbol{\mu}}_s}{\sigma \|\hat{\boldsymbol{\mu}}_s\|_{\ell_2}}\right).
\end{aligned} \tag{21}
$$

Here Q-function is the tail distribution function of the standard normal distribution.

Next, similarly, given that $\boldsymbol{x}_i \sim \mathcal{N}(y_i \cdot \boldsymbol{\mu}, \sigma^2 \boldsymbol{I})$ for $i \in \mathcal{I}$, we can rewrite

$$
\hat{\boldsymbol{\mu}}_s = \frac{1}{m} \sum_{i \in \mathcal{I}} y_i \boldsymbol{x}_i = \boldsymbol{\mu} + \frac{\sigma}{\sqrt{m}} \boldsymbol{g}_2 \quad \text{where} \quad \boldsymbol{g}_2 \sim \mathcal{N}(0, \boldsymbol{I}).
$$

Then combining (20) and (21), we have

$$\begin{aligned}\mathbb{P}(y^\star_{\text{att-1}}(\boldsymbol{Z}) \neq y) &= \mathbb{E}_{\boldsymbol{\mu},\boldsymbol{g}_2}\left[Q\left(\frac{\boldsymbol{\mu}^\top \hat{\boldsymbol{\mu}}_s}{\sigma \left\|\hat{\boldsymbol{\mu}}_s\right\|_{\ell_2}}\right)\right] \\ &= \mathbb{E}_{\boldsymbol{\mu},\boldsymbol{g}_2}\left[Q\left(\frac{\boldsymbol{\mu}^\top(\boldsymbol{\mu}+\frac{\sigma}{\sqrt{m}}\boldsymbol{g}_2)}{\sigma\left\|\boldsymbol{\mu}+\frac{\sigma}{\sqrt{m}}\boldsymbol{g}_2\right\|_{\ell_2}}\right)\right] \\ &= \mathbb{E}_{\boldsymbol{\mu},\boldsymbol{g}_2}\left[Q\left(\frac{1+\frac{\sigma}{\sqrt{m}}\boldsymbol{\mu}^\top\boldsymbol{g}_2}{\sigma\sqrt{1+2\frac{\sigma}{\sqrt{m}}\boldsymbol{\mu}^\top\boldsymbol{g}_2+\frac{\sigma^2}{m}\left\|\boldsymbol{g}_2\right\|_{\ell_2}^2}}\right)\right].\end{aligned}$$

Note that for any $\boldsymbol{\mu}$ with $\|\boldsymbol{\mu}\|_{\ell_2}=1$, we have $\boldsymbol{\mu}^\top\boldsymbol{g}_2 \sim \mathcal{N}(0,1)$. Therefore, we can write

$$\boldsymbol{\mu}^\top\boldsymbol{g}_2 = g \quad \text{where} \quad g\sim\mathcal{N}(0,1),$$

and let $\boldsymbol{U}\in\mathbb{R}^{d\times d}$ be a unitary matrix with first row being $\boldsymbol{\mu}$. We can write

$$\|\boldsymbol{g}_2\|_{\ell_2}^2 = \|\boldsymbol{U}\boldsymbol{g}_2\|_{\ell_2}^2 = g^2+h \quad \text{where} \quad h\sim\mathcal{X}^2_{d-1}.$$

Here, $\mathcal{X}^2_{d-1}$ denotes chi-squared distribution with $(d-1)$ degrees of freedom. Then, we get

$$\begin{aligned}\mathbb{P}(y^\star_{\text{att-1}}(\boldsymbol{Z}) \neq y) &= \mathbb{E}_{g,h}\left[Q\left(\frac{1+\frac{\sigma}{\sqrt{m}}g}{\sigma\sqrt{1+2\frac{\sigma}{\sqrt{m}}g+\frac{\sigma^2}{m}(g^2+h)}}\right)\right] \\ &= \mathbb{E}_{g,h}\left[Q\left(\frac{1+\frac{\sigma}{\sqrt{m}}g}{\sigma\sqrt{(1+\frac{\sigma}{\sqrt{m}}g)^2+\frac{\sigma^2}{m}h}}\right)\right], \\ &= \mathbb{E}_{g,h}\left[Q\left(\frac{1+\varepsilon_\sigma g}{\sigma\sqrt{(1+\varepsilon_\sigma g)^2+\varepsilon_\sigma^2 h}}\right)\right],\end{aligned}$$

where $\varepsilon_\sigma := \sigma/\sqrt{m}$. It completes the proof of (7).

Next, we derive an upper bound for $\mathbb{P}(y^\star_{\text{att-1}}(\boldsymbol{Z}) \neq y)$. Let $c := \varepsilon_\sigma^{-1}$. Then we have

$$\begin{aligned}\mathbb{P}(y^\star_{\text{att-1}}(\boldsymbol{Z}) \neq y) &= \mathbb{E}_{g,h}\left[Q\left(\frac{c+g}{\sigma\sqrt{(c+g)^2+h}}\right)\right] \\ &= \mathbb{E}_{g\geq-\frac{c}{2},h}\left[Q\left(\frac{c+g}{\sigma\sqrt{(c+g)^2+h}}\right)\right] + \mathbb{E}_{g<-\frac{c}{2},h}\left[Q\left(\frac{c+g}{\sigma\sqrt{(c+g)^2+h}}\right)\right] \\ &\leq \mathbb{E}_{g\geq-\frac{c}{2},h}\left[Q\left(\frac{c+g}{\sigma\sqrt{(c+g)^2+h}}\right)\right] + Q(c/2) \\ &= \mathbb{E}_{g\geq-\frac{c}{2},h}\left[Q\left(\frac{1}{\sigma\sqrt{1+h/(c+g)^2}}\right)\right] + Q(c/2), \qquad (22)\end{aligned}$$

where the inequality comes from the fact that $\mathbb{P}(g\leq -c/2) = Q(c/2)$ and $Q(x)\leq 1$ for any $x\in\mathbb{R}$, and we have

$$\frac{1}{\sqrt{1+h/(c+g)^2}} \geq 1-\frac{1}{2}\frac{h}{(c+g)^2} \geq 1-\frac{2h}{c^2}.$$

Here the first inequality comes from that $\frac{1}{\sqrt{1+x}}\geq 1-\frac{1}{2}x$ and the second utilizes that $g\geq-\frac{c}{2}$.

Since $h \sim \mathcal{X}^2_{d-1}$, from the Laurent-Massart inequality (Laurent & Massart, 2000), we have that

$$\mathbb{P}\left(h \geq d - 1 + 2\sqrt{(d-1)t_1} + 2t_1\right) \leq e^{-t_1}.$$

Therefore, we have that with probability at least $1 - e^{-t_1}$

$$\frac{1}{\sqrt{1 + h/(c+g)^2}} \geq 1 - \frac{2(d - 1 + 2\sqrt{(d-1)t_1} + 2t_1)}{c^2}.$$

Setting $t_1 = d$, we get

$$\frac{1}{\sqrt{1 + h/(c+g)^2}} \geq 1 - \frac{10d}{c^2}.$$

Combining the result with (22), since $Q(x) \leq 1$ for $x \in \mathbb{R}$ and $Q(x) \leq e^{-x^2/2}$ for $x > 1$, we get that

$$\begin{aligned}\mathbb{P}(y^\star_{\text{att-1}}(\boldsymbol{Z}) \neq y) &\leq e^{-d} + Q(c/2) + Q\left(\frac{1}{\sigma}\left(1 - \frac{10d}{c^2}\right)\right) \\ &\leq e^{-d} + e^{-1/8\varepsilon_\sigma^2} + Q\left(\frac{1}{\sigma}\left(1 - 10d\varepsilon_\sigma^2\right)\right).\end{aligned}$$

It completes the proof.

□

E. Analysis of Multi-layer Linear Attention

E.1. Proof of Proposition 4.1

Proof. We consider the following model constructions for the attention matrices in the ℓ'th layer, $\ell \in [L]$ and the final linear prediction head:

$$\begin{aligned}\ell\text{'th layer:} \quad \boldsymbol{W}_{q\ell}\boldsymbol{W}_{k\ell}^\top &= \begin{bmatrix}\boldsymbol{I}_d & 0\\ 0 & 0\end{bmatrix} \quad \text{and} \quad \boldsymbol{W}_{v\ell} = \begin{bmatrix}a_\ell \boldsymbol{I}_d & 0\\ 0 & b_\ell\end{bmatrix}; \\ \text{Prediction head:} \quad \boldsymbol{h} &= \begin{bmatrix}\boldsymbol{0}_d \\ c\end{bmatrix}.\end{aligned} \tag{23}$$

Suppose the input to ℓ'th layer is

$$\boldsymbol{Z}_\ell = \begin{bmatrix}\boldsymbol{X}_\ell & \boldsymbol{y}_\ell \\ \boldsymbol{x}_\ell^\top & y_\ell\end{bmatrix} \in \mathbb{R}^{(n+1)\times(d+1)} \quad \text{where} \quad \boldsymbol{Z}_1 = \boldsymbol{Z} = \begin{bmatrix}\boldsymbol{X} & \boldsymbol{y} \\ \boldsymbol{x}^\top & 0\end{bmatrix}.$$

Recapping the model construction from (23), the ℓ'th layer output returns

$$\begin{aligned}\left(\boldsymbol{Z}_\ell \boldsymbol{W}_{q\ell}\boldsymbol{W}_{k\ell}^\top \boldsymbol{Z}_\ell^\top \boldsymbol{M}\right)\boldsymbol{Z}_\ell \boldsymbol{W}_{v\ell} &= \begin{bmatrix}\boldsymbol{X}_\ell & \boldsymbol{y}_\ell \\ \boldsymbol{x}_\ell^\top & y_\ell\end{bmatrix}\begin{bmatrix}\boldsymbol{I}_d & 0\\ 0 & 0\end{bmatrix}\begin{bmatrix}\boldsymbol{X}_\ell^\top & \boldsymbol{x}_\ell \\ \boldsymbol{y}_\ell^\top & y_\ell\end{bmatrix}\boldsymbol{M}\begin{bmatrix}\boldsymbol{X}_\ell & \boldsymbol{y}_\ell \\ \boldsymbol{x}_\ell^\top & y_\ell\end{bmatrix}\begin{bmatrix}a_\ell \boldsymbol{I}_d & 0\\ 0 & b_\ell\end{bmatrix} \\ &= \begin{bmatrix}\boldsymbol{X}_\ell \boldsymbol{X}_\ell^\top & \boldsymbol{X}_\ell \boldsymbol{x}_\ell \\ \boldsymbol{x}_\ell^\top \boldsymbol{X}_\ell^\top & \boldsymbol{x}_\ell^\top \boldsymbol{x}_\ell\end{bmatrix}\begin{bmatrix}\boldsymbol{I}_n & 0\\ 0 & 0\end{bmatrix}\begin{bmatrix}a_\ell \boldsymbol{X}_\ell & b_\ell \boldsymbol{y}_\ell \\ a_\ell \boldsymbol{x}_\ell^\top & b_\ell y_\ell\end{bmatrix} \\ &= \begin{bmatrix}a_\ell \boldsymbol{X}_\ell \boldsymbol{X}_\ell^\top \boldsymbol{X}_\ell & b_\ell \boldsymbol{X}_\ell \boldsymbol{X}_\ell^\top \boldsymbol{y}_\ell \\ a_\ell \boldsymbol{x}_\ell^\top \boldsymbol{X}_\ell^\top \boldsymbol{X}_\ell & b_\ell \boldsymbol{x}_\ell^\top \boldsymbol{X}_\ell^\top \boldsymbol{y}_\ell\end{bmatrix}.\end{aligned} \tag{24}$$

Therefore, the input of $(\ell+1)$'th layer is

$$\begin{aligned}\boldsymbol{Z}_{\ell+1} &= \boldsymbol{Z}_\ell + \begin{bmatrix}a_\ell \boldsymbol{X}_\ell \boldsymbol{X}_\ell^\top \boldsymbol{X}_\ell & b_\ell \boldsymbol{X}_\ell \boldsymbol{X}_\ell^\top \boldsymbol{y}_\ell \\ a_\ell \boldsymbol{x}_\ell^\top \boldsymbol{X}_\ell^\top \boldsymbol{X}_\ell & b_\ell \boldsymbol{x}_\ell^\top \boldsymbol{X}_\ell^\top \boldsymbol{y}_\ell\end{bmatrix} \\ &= \begin{bmatrix}\boldsymbol{X}_\ell + a_\ell \boldsymbol{X}_\ell \boldsymbol{X}_\ell^\top \boldsymbol{X}_\ell & \boldsymbol{y}_\ell + b_\ell \boldsymbol{X}_\ell \boldsymbol{X}_\ell^\top \boldsymbol{y}_\ell \\ \boldsymbol{x}_\ell^\top + a_\ell \boldsymbol{x}_\ell^\top \boldsymbol{X}_\ell^\top \boldsymbol{X}_\ell & y_\ell + b_\ell \boldsymbol{x}_\ell^\top \boldsymbol{X}_\ell^\top \boldsymbol{y}_\ell\end{bmatrix} \in \mathbb{R}^{(n+1)\times(d+1)}.\end{aligned} \tag{25}$$

• **Label propagation:** We first focus on deriving label propagation results. Suppose that we have

$$a_\ell = 0 \quad \text{for} \quad \ell \in [L].$$

Then following (24), the output of ℓ'th layer takes the following form:

$$\left(\boldsymbol{Z}_\ell \boldsymbol{W}_{q\ell} \boldsymbol{W}_{k\ell}^\top \boldsymbol{Z}_\ell^\top M\right) \boldsymbol{Z}_\ell \boldsymbol{W}_{v\ell} = \begin{bmatrix} 0 & b_\ell \boldsymbol{X}_\ell \boldsymbol{X}_\ell^\top \boldsymbol{y}_\ell \\ 0 & b_\ell \boldsymbol{x}_\ell^\top \boldsymbol{X}_\ell^\top \boldsymbol{y}_\ell \end{bmatrix}.$$

Here, the first d coordinates of each token's output are zeros, and therefore, the corresponding input coordinates remain unchanged, and we have

$$\boldsymbol{X}_\ell \equiv \boldsymbol{X} \quad \text{and} \quad \boldsymbol{x}_\ell \equiv \boldsymbol{x} \quad \text{for} \quad \ell \in [L].$$

The prediction (based on the last token output and after applying prediction head) is given by

$$f_{\text{all-}L}(\boldsymbol{Z}) = c b_L \boldsymbol{x}^\top \boldsymbol{X}^\top \boldsymbol{y}_L. \tag{26}$$

We next focus on obtaining $\boldsymbol{y}_L$. From (25), we have

$$\boldsymbol{y}_{\ell+1} = \boldsymbol{y}_\ell + b_\ell \boldsymbol{X}\boldsymbol{X}^\top \boldsymbol{y}_\ell = (\boldsymbol{I} + b_\ell \boldsymbol{X}\boldsymbol{X}^\top)\boldsymbol{y}_\ell.$$

Therefore,

$$\boldsymbol{y}_L = \prod_{\ell=1}^{L-1} (\boldsymbol{I} + b_\ell \boldsymbol{X}\boldsymbol{X}^\top)\boldsymbol{y}.$$

Combining with (26) results in

$$f_{\text{all-}L}(\boldsymbol{Z}) = c b_L \boldsymbol{x}^\top \boldsymbol{X}^\top \prod_{\ell=1}^{L-1} (\boldsymbol{I} + b_\ell \boldsymbol{X}\boldsymbol{X}^\top)\boldsymbol{y} = c b_L \boldsymbol{x}^\top \prod_{\ell=1}^{L-1} (\boldsymbol{I} + b_\ell \boldsymbol{X}^\top\boldsymbol{X})\boldsymbol{X}^\top \boldsymbol{y}.$$

It completes the proof.

• **Feature propagation:** We now focus on the feature propagation setting. In contrast to the label propagation, let us assume that

$$a_\ell \to \infty \quad \text{and} \quad b_\ell \to 0^+ \quad \text{for} \quad \ell \in [L].$$

The prediction (following (24), based on the last token output and after applying prediction head) is given by

$$f_{\text{all-}L}(\boldsymbol{Z}) = c b_L \boldsymbol{x}_L^\top \boldsymbol{X}_L^\top \boldsymbol{y}_L. \tag{27}$$

We first obtain $\boldsymbol{y}_L$. From (25) (since $b_\ell \to 0$), we have

$$\boldsymbol{y}_{\ell+1} = \boldsymbol{y}_\ell + b_\ell \boldsymbol{X}\boldsymbol{X}^\top \boldsymbol{y}_\ell = \boldsymbol{y}_\ell.$$

Therefore,

$$\boldsymbol{y}_L = \boldsymbol{y}.$$

Next, we focus on $\boldsymbol{X}_L, \boldsymbol{x}_L$. From (25), as $a_\ell \to \infty$, we have

$$\boldsymbol{X}_{\ell+1} = \boldsymbol{X}_\ell + a_\ell \boldsymbol{X}_\ell \boldsymbol{X}_\ell^\top \boldsymbol{X}_\ell = \boldsymbol{X}_\ell(\boldsymbol{I} + a_\ell \boldsymbol{X}_\ell^\top \boldsymbol{X}_\ell) = a_\ell \boldsymbol{X}_\ell \boldsymbol{X}_\ell^\top \boldsymbol{X}_\ell;$$
$$\boldsymbol{x}_{\ell+1}^\top = \boldsymbol{x}_\ell^\top + a_\ell \boldsymbol{x}_\ell^\top \boldsymbol{X}_\ell^\top \boldsymbol{X}_\ell = \boldsymbol{x}_\ell^\top (\boldsymbol{I} + a_\ell \boldsymbol{X}_\ell^\top \boldsymbol{X}_\ell) = a_\ell \boldsymbol{x}_\ell^\top \boldsymbol{X}_\ell^\top \boldsymbol{X}_\ell.$$

Therefore,

$$\begin{aligned}\boldsymbol{X}_L &= a_{L-1}\boldsymbol{X}_{L-1}(\boldsymbol{X}_{L-1}^\top \boldsymbol{X}_{L-1}) \\ &= a_{L-1}a_{L-2}^3\boldsymbol{X}_{L-2}(\boldsymbol{X}_{L-2}^\top \boldsymbol{X}_{L-2})^{\frac{3^2-1}{2}} \\ &= a_{L-1}a_{L-2}^3 a_{L-3}^{3^2}\boldsymbol{X}_{L-3}(\boldsymbol{X}_{L-3}^\top \boldsymbol{X}_{L-3})^{\frac{3^3-1}{2}} \\ &= \cdots \\ &= a_{L-1}a_{L-2}^3 a_{L-3}^{3^2}...a_1^{3^{L-2}}\boldsymbol{X}(\boldsymbol{X}^\top \boldsymbol{X})^{\frac{3^{L-1}-1}{2}},\end{aligned}$$

and

$$\begin{aligned}\boldsymbol{x}_L^\top &= a_{L-1}\boldsymbol{x}_{L-1}^\top(\boldsymbol{X}_{L-1}^\top \boldsymbol{X}_{L-1}) \\ &= a_{L-1}a_{L-2}^3\boldsymbol{x}_{L-2}^\top(\boldsymbol{X}_{L-2}^\top \boldsymbol{X}_{L-2})^{\frac{3^2-1}{2}} \\ &= a_{L-1}a_{L-2}^3 a_{L-3}^{3^2}\boldsymbol{x}_{L-3}^\top(\boldsymbol{X}_{L-3}^\top \boldsymbol{X}_{L-3})^{\frac{3^3-1}{2}} \\ &= \cdots \\ &= a_{L-1}a_{L-2}^3 a_{L-3}^{3^2}...a_1^{3^{L-2}}\boldsymbol{x}^\top(\boldsymbol{X}^\top \boldsymbol{X})^{\frac{3^{L-1}-1}{2}}.\end{aligned}$$

Combining all together with (27), we have that

$$\begin{aligned}f_{\text{all-}L}(\boldsymbol{Z}) &= cb_L\boldsymbol{x}_L^\top \boldsymbol{X}_L^\top \boldsymbol{y}_L \\ &= cb_L\left(\prod_{\ell=1}^{L-1} a_\ell^{3^{L-1-\ell}}\right)^2 \boldsymbol{x}^\top(\boldsymbol{X}^\top \boldsymbol{X})^{3^{L-1}-1}\boldsymbol{X}^\top \boldsymbol{y}.\end{aligned}$$

It completes the proof. □

E.2. Proof of Proposition 4.2

Proof. The proof follows directly by adopting the same model construction and proof strategy as in Proposition 4.1, under the additional assumption that

$$a_\ell = a \quad \text{and} \quad b_\ell = b \quad \text{for} \quad \ell \in [L].$$

□

E.3. Proof of Lemma 4.3

Proof. In the proof of Proposition 4.1, we showed how to derive the label and feature propagation results by restricting the construction to either $a_\ell \equiv 0$ (for label propagation) or $(a_\ell \to \infty, b_\ell \to 0)$ (for feature propagation). Here, we consider a propagation process without imposing restrictions on the choices of (a_ℓ, b_ℓ), and study the form of the final prediction returned by the model.

To avoid the notation conflict, we express the matrix $\boldsymbol{A}$ in (10) as

$$\boldsymbol{A} = \sum_{k=0}^{K} e_k(\boldsymbol{X}^\top \boldsymbol{X})^k$$

and let $\boldsymbol{e} = [e_0\ e_2\ \cdots\ e_{(3^L-3)/2}]^\top \in \mathbb{R}^{K+1}$.

Recall the same model construction used in the proof of Proposition 4.1, defined in (23). From (24), we have that

$$f_{\text{att-}L}(\boldsymbol{Z}) = cb_L\boldsymbol{x}_L^\top \boldsymbol{X}_L^\top \boldsymbol{y}_L$$

where following (25), we have

$$\begin{aligned}\boldsymbol{X}_{\ell+1} &= (\boldsymbol{I} + a_\ell \boldsymbol{X}_\ell \boldsymbol{X}_\ell^\top)\boldsymbol{X}_\ell, \\ \boldsymbol{x}_{\ell+1}^\top &= \boldsymbol{x}_\ell^\top(\boldsymbol{I} + a_\ell \boldsymbol{X}_\ell^\top \boldsymbol{X}_\ell), \\ \boldsymbol{y}_{\ell+1} &= (\boldsymbol{I} + b_\ell \boldsymbol{X}_\ell \boldsymbol{X}_\ell^\top)\boldsymbol{y}_\ell.\end{aligned}$$

At each layer, the operations performed are linear combinations and multiplications involving $\boldsymbol{X}_\ell^\top \boldsymbol{X}_\ell$ and identity matrices scaled by the parameters (a_ℓ, b_ℓ). Thus, each coefficient e_k of $(\boldsymbol{X}^\top \boldsymbol{X})^k$ depends smoothly on the scalar parameters (a_ℓ, b_ℓ).

From (24) and (25), we have that

$$\begin{aligned} f_{\text{att-}L}(\boldsymbol{Z}) &= cb_L \boldsymbol{x}_L^\top \boldsymbol{X}_L^\top \boldsymbol{y}_L \\ &= cb_L \cdot \boldsymbol{x}_{L-1}^\top (\boldsymbol{I} + a_{L-1}\boldsymbol{X}_{L-1}^\top \boldsymbol{X}_{L-1})(\boldsymbol{I} + a_{L-1}\boldsymbol{X}_{L-1}^\top \boldsymbol{X}_{L-1})\boldsymbol{X}_{L-1}^\top \cdot (\boldsymbol{I} + b_{L-1}\boldsymbol{X}_{L-1}\boldsymbol{X}_{L-1}^\top)\boldsymbol{y}_{L-1} \\ &= \cdots \end{aligned} \tag{28}$$

That is, in the final $f_{\text{att-}L}(\boldsymbol{Z})$ expression, the coefficients corresponding to different degrees of $(\boldsymbol{X}^\top \boldsymbol{X})^k$ depend on the model parameters cb_L and $(a_\ell, b_\ell)_{\ell=1}^{L-1}$, which together have at most $2L-1$ degrees of freedom. Let $\boldsymbol{c} = [cb_L\ a_1\ \cdots\ a_{L-1}\ b_1\ \cdots\ b_{L-1}]^\top$. This means there exists a smooth function $g : \mathbb{R}^{2L-1} \to \mathbb{R}^K$ such that: $\boldsymbol{e} = g(\boldsymbol{c})$.

It remains to show that an L-layer linear attention model can produce terms involving powers of $\boldsymbol{X}^\top \boldsymbol{X}$ up to degree $(3^L - 3)/2$.

Let $f(\boldsymbol{Z})$ be a function that contains terms of the form $\boldsymbol{X}^\top (\boldsymbol{X}^\top \boldsymbol{X})^k \boldsymbol{X}^\top \boldsymbol{y}$ for various powers k. Define $\mathcal{P}(f(\boldsymbol{Z}))$ as the projection that extracts the highest degree k present in $f(\boldsymbol{Z})$. For example, $\mathcal{P}\big(\boldsymbol{x}^\top (\boldsymbol{I} + (\boldsymbol{X}^\top \boldsymbol{X})^2)\boldsymbol{X}^\top \boldsymbol{y}\big) = 2$. Then from (28), we have

$$\begin{aligned} \mathcal{P}(f_{\text{att-}L}(\boldsymbol{Z})) &= \mathcal{P}(\boldsymbol{x}_L^\top \boldsymbol{X}_L^\top \boldsymbol{y}_L) \\ &= \mathcal{P}(\boldsymbol{x}_{L-1}^\top (\boldsymbol{X}_{L-1}^\top \boldsymbol{X}_{L-1})^3 \boldsymbol{X}_{L-1}^\top \boldsymbol{y}_{L-1}) \\ &= \mathcal{P}(\boldsymbol{x}_{L-2}^\top (\boldsymbol{X}_{L-2}^\top \boldsymbol{X}_{L-2})(\boldsymbol{X}_{L-2}^\top \boldsymbol{X}_{L-2})^{3^2} (\boldsymbol{X}_{L-2}^\top \boldsymbol{X}_{L-2})^2 \boldsymbol{X}_{L-2}^\top \boldsymbol{y}_{L-2}) \\ &= \mathcal{P}(\boldsymbol{x}_{L-2}^\top (\boldsymbol{X}_{L-2}^\top \boldsymbol{X}_{L-2})^{3^2+3} \boldsymbol{X}_{L-2}^\top \boldsymbol{y}_{L-2}) \\ &= \mathcal{P}(\boldsymbol{x}_{L-3}^\top (\boldsymbol{X}_{L-3}^\top \boldsymbol{X}_{L-3})(\boldsymbol{X}_{L-3}^\top \boldsymbol{X}_{L-3})^{3^3+3^2} (\boldsymbol{X}_{L-3}^\top \boldsymbol{X}_{L-3})^2 \boldsymbol{X}_{L-3}^\top \boldsymbol{y}_{L-3}) \\ &= \mathcal{P}(\boldsymbol{x}_{L-3}^\top (\boldsymbol{X}_{L-3}^\top \boldsymbol{X}_{L-3})^{3^3+3^2+3} \boldsymbol{X}_{L-3}^\top \boldsymbol{y}_{L-3}) \\ &= \cdots \\ &= \mathcal{P}(\boldsymbol{x}^\top (\boldsymbol{X}^\top \boldsymbol{X})^{3^{L-1}+\cdots+3^2+3} \boldsymbol{X}^\top \boldsymbol{y}) \\ &= 3^{L-1} + \cdots + 3^2 + 3 = \frac{3^L - 3}{2}. \end{aligned}$$

It completes the proof.

□

E.4. Proof of Theorem 4.4

Proof. Let $\boldsymbol{\xi} \sim \mathcal{N}(0, \boldsymbol{I})$ and rewrite $y\boldsymbol{x} = \boldsymbol{\mu} + \sigma\boldsymbol{\xi}$. For any matrix $\boldsymbol{A} \in \mathbb{R}^{d\times d}$, the prediction error of $\hat{y}_{\boldsymbol{A}} = \operatorname{sgn}(\boldsymbol{x}^\top \boldsymbol{A}\hat{\boldsymbol{\mu}}_s)$ given $\hat{\boldsymbol{\mu}}_s$ returns

$$\begin{aligned} \mathbb{P}(\hat{\boldsymbol{y}}_{\boldsymbol{A}} \neq y \mid \hat{\boldsymbol{\mu}}_s) &= \mathbb{P}(y\boldsymbol{x}^\top \boldsymbol{A}\hat{\boldsymbol{\mu}}_s < 0 \mid \hat{\boldsymbol{\mu}}_s) \\ &= \mathbb{P}((\boldsymbol{\mu} + \sigma\boldsymbol{\xi})^\top \boldsymbol{A}\hat{\boldsymbol{\mu}}_s < 0 \mid \hat{\boldsymbol{\mu}}_s) \\ &= Q\left(\frac{\boldsymbol{\mu}^\top \boldsymbol{A}\hat{\boldsymbol{\mu}}_s}{\sigma \left\|\boldsymbol{A}\hat{\boldsymbol{\mu}}_s\right\|_{\ell_2}}\right). \end{aligned} \tag{29}$$

For any $\boldsymbol{A} \in \mathbb{R}^{d\times d}$, we can decompose it as

$$\boldsymbol{A} = \sum_{i=1}^{d} \lambda_i \boldsymbol{u}_i \boldsymbol{v}_i^\top$$

where $\boldsymbol{u}_1 = \boldsymbol{\mu}$, $\|\boldsymbol{u}_i\|_{\ell_2} = 1$ and $\boldsymbol{u}_i^\top \boldsymbol{u}_j = 0$ for any $i \neq j$. Let $\lambda_1 > 0$. Then, we get

$$\begin{aligned}\boldsymbol{\mu}^\top \boldsymbol{A}\hat{\boldsymbol{\mu}}_s &= \boldsymbol{\mu}^\top (\sum_{i=1}^{d} \lambda_i \boldsymbol{u}_i \boldsymbol{v}_i^\top)\hat{\boldsymbol{\mu}}_s \\ &= \sum_{i=1}^{d} \lambda_i \boldsymbol{\mu}^\top \boldsymbol{u}_i \boldsymbol{v}_i^\top \hat{\boldsymbol{\mu}}_s \\ &= \lambda_1 \boldsymbol{\mu}^\top \boldsymbol{u}_1 \boldsymbol{v}_1^\top \hat{\boldsymbol{\mu}}_s \\ &= \lambda_1 \boldsymbol{v}_1^\top \hat{\boldsymbol{\mu}}_s. \end{aligned} \tag{30}$$

Now consider $\|\boldsymbol{A}\hat{\boldsymbol{\mu}}_s\|_{\ell_2}$ where we have

$$\begin{aligned}\boldsymbol{A}\hat{\boldsymbol{\mu}}_s &= \sum_{i=1}^{d} \lambda_i \boldsymbol{u}_i \boldsymbol{v}_i^\top \hat{\boldsymbol{\mu}}_s \\ &= \lambda_1 \boldsymbol{\mu} \boldsymbol{v}_1^\top \hat{\boldsymbol{\mu}}_s + \sum_{i=2}^{d} \lambda_i \boldsymbol{u}_i \boldsymbol{v}_i^\top \hat{\boldsymbol{\mu}}_s. \end{aligned}$$

Since $\boldsymbol{u}_i$, $i \neq 1$ is orthogonal to $\boldsymbol{\mu}$, $\lambda_1 \boldsymbol{\mu} \boldsymbol{v}_1^\top \hat{\boldsymbol{\mu}}_s$ is orthogonal to $\sum_{i=2}^{d} \lambda_i \boldsymbol{u}_i \boldsymbol{v}_i^\top \hat{\boldsymbol{\mu}}_s$. Therefore, given $\|\boldsymbol{u}_i\|_{\ell_2} = 1$ for all $i \in [d]$, it obeys

$$\|\boldsymbol{A}\hat{\boldsymbol{\mu}}_s\|_{\ell_2}^2 = \left\|\lambda_1 \boldsymbol{\mu} \boldsymbol{v}_1^\top \hat{\boldsymbol{\mu}}_s\right\|_{\ell_2}^2 + \sum_{i=2}^{d} \left\|\lambda_i \boldsymbol{u}_i \boldsymbol{v}_i^\top \hat{\boldsymbol{\mu}}_s\right\|_{\ell_2}^2 = (\lambda_1 \boldsymbol{v}_1^\top \hat{\boldsymbol{\mu}}_s)^2 + \lambda_1^2 \sum_{i=2}^{d} (\lambda_1^{-1} \lambda_i \boldsymbol{v}_i^\top \hat{\boldsymbol{\mu}}_s)^2. \tag{31}$$

For simplicity, define

$$\Delta(\hat{\boldsymbol{\mu}}_s) = \sum_{i=2}^{d} (\lambda_1^{-1} \lambda_i \boldsymbol{v}_i^\top \hat{\boldsymbol{\mu}}_s)^2$$

where we have

$$\Delta(\hat{\boldsymbol{\mu}}_s) \geq 0 \quad \text{and} \quad \Delta(-\hat{\boldsymbol{\mu}}_s) = \Delta(\hat{\boldsymbol{\mu}}_s).$$

Recall that $\hat{\boldsymbol{\mu}}_s$ is the SPI estimator (cf. (SPI)). Let $|\mathcal{I}| = m$. We can write $\hat{\boldsymbol{\mu}}_s = \boldsymbol{\mu} + \frac{\sigma}{\sqrt{m}} \boldsymbol{\xi}'$ where $\boldsymbol{\xi}' \sim \mathcal{N}(0, \boldsymbol{I})$.

Using (29), (30) and (31), the classification error becomes

$$\begin{aligned}\mathbb{P}(\hat{\boldsymbol{y}}_{\boldsymbol{A}} \neq y) &= \mathbb{E}_{\hat{\boldsymbol{\mu}}_s}\left[Q\left(\frac{\boldsymbol{\mu}^\top \boldsymbol{A}\hat{\boldsymbol{\mu}}_s}{\sigma \|\boldsymbol{A}\hat{\boldsymbol{\mu}}_s\|_{\ell_2}}\right)\right] \\ &= \mathbb{E}_{\hat{\boldsymbol{\mu}}_s}\left[Q\left(\frac{\boldsymbol{v}_1^\top \hat{\boldsymbol{\mu}}_s}{\sigma\sqrt{(\boldsymbol{v}_1^\top \hat{\boldsymbol{\mu}}_s)^2 + \Delta(\hat{\boldsymbol{\mu}}_s)}}\right)\right]. \end{aligned}$$

First, note that for any $x > 0$, $Q(x) < 0.5 < Q(-x)$. Therefore, the optimal $\boldsymbol{v}_1 \in \mathbb{R}^d$ maximizes $\mathbb{P}(\boldsymbol{v}_1^\top \hat{\boldsymbol{\mu}}_s > 0)$. Let $\boldsymbol{v}_1^\star := \arg\max_{\boldsymbol{v}_1 \in \mathbb{R}^d} \mathbb{P}(\boldsymbol{v}_1^\top \hat{\boldsymbol{\mu}}_s > 0)$. Given that $\hat{\boldsymbol{\mu}}_s \sim \mathcal{N}(\boldsymbol{\mu}, \sigma^2/m\boldsymbol{I})$, we have that $\boldsymbol{v}_1^\star = c\boldsymbol{\mu}$ for $c > 0$. Let $c = 1$ and therefore, $\boldsymbol{v}_1^\star = \boldsymbol{\mu}$ without loss of generality. Then we obtain

$$\mathbb{P}(\hat{\boldsymbol{y}}_{\boldsymbol{A}} \neq y) = \mathbb{E}_{\hat{\boldsymbol{\mu}}_s}\left[Q\left(\frac{\boldsymbol{\mu}^\top \hat{\boldsymbol{\mu}}_s}{\sigma\sqrt{(\boldsymbol{\mu}^\top \hat{\boldsymbol{\mu}}_s)^2 + \Delta(\hat{\boldsymbol{\mu}}_s)}}\right)\right].$$

Let $f(\hat{\boldsymbol{\mu}}_s)$ be the probability density function of $\hat{\boldsymbol{\mu}}_s$. Since $\hat{\boldsymbol{\mu}}_s \sim \mathcal{N}(\boldsymbol{\mu}, \sigma^2/m\boldsymbol{I})$, then it satisfies

$$f(\hat{\boldsymbol{\mu}}_s) \geq f(-\hat{\boldsymbol{\mu}}_s) \quad \text{for any } \boldsymbol{\mu}^\top \hat{\boldsymbol{\mu}}_s > 0. \tag{32}$$

Therefore, the classification error becomes

$$\begin{aligned}\mathbb{P}(\hat{\boldsymbol{y}}_{\boldsymbol{A}} \neq y) &= \int_{\hat{\boldsymbol{\mu}}_s} f(\hat{\boldsymbol{\mu}}_s) Q\left(\frac{\boldsymbol{\mu}^\top \hat{\boldsymbol{\mu}}_s}{\sigma\sqrt{(\boldsymbol{\mu}^\top \hat{\boldsymbol{\mu}}_s)^2 + \Delta(\hat{\boldsymbol{\mu}}_s)}}\right) d\hat{\boldsymbol{\mu}}_s \\ &= \int_{\boldsymbol{\mu}^\top \hat{\boldsymbol{\mu}}_s > 0} f(\hat{\boldsymbol{\mu}}_s) Q\left(\frac{\boldsymbol{\mu}^\top \hat{\boldsymbol{\mu}}_s}{\sigma\sqrt{(\boldsymbol{\mu}^\top \hat{\boldsymbol{\mu}}_s)^2 + \Delta(\hat{\boldsymbol{\mu}}_s)}}\right) + f(-\hat{\boldsymbol{\mu}}_s) Q\left(\frac{-\boldsymbol{\mu}^\top \hat{\boldsymbol{\mu}}_s}{\sigma\sqrt{(\boldsymbol{\mu}^\top \hat{\boldsymbol{\mu}}_s)^2 + \Delta(\hat{\boldsymbol{\mu}}_s)}}\right) d\hat{\boldsymbol{\mu}}_s \\ &= \int_{\boldsymbol{\mu}^\top \hat{\boldsymbol{\mu}}_s > 0} \left(f(\hat{\boldsymbol{\mu}}_s) - f(-\hat{\boldsymbol{\mu}})\right) Q\left(\frac{\boldsymbol{\mu}^\top \hat{\boldsymbol{\mu}}_s}{\sigma\sqrt{(\boldsymbol{\mu}^\top \hat{\boldsymbol{\mu}}_s)^2 + \Delta(\hat{\boldsymbol{\mu}}_s)}}\right) + f(-\hat{\boldsymbol{\mu}}_s) d\hat{\boldsymbol{\mu}}_s.\end{aligned}$$

Following (32), to minimize the error, we need minimize $Q\left(\frac{\boldsymbol{\mu}^\top \hat{\boldsymbol{\mu}}_s}{\sigma\sqrt{(\boldsymbol{\mu}^\top \hat{\boldsymbol{\mu}}_s)^2 + \Delta(\hat{\boldsymbol{\mu}}_s)}}\right)$ for $\boldsymbol{\mu}^\top \hat{\boldsymbol{\mu}}_s > 0$, which can be easily done by choosing $\lambda_i = 0$ for $i \geq 2$. Then we get $\Delta(\hat{\boldsymbol{\mu}}_s) \equiv 0$. Therefore, the optimal solution set $\mathcal{A}^\star$ defined in Theorem 4.4 satisfies:

$$\mathcal{A}^\star = \left\{\lambda_1 \boldsymbol{\mu}\boldsymbol{\mu}^\top \;\middle|\; \lambda_1 > 0\right\}.$$

Combining all together, we obtain

$$\begin{aligned}\mathbb{P}(\hat{\boldsymbol{y}}_{\boldsymbol{A}} \neq y) &= \int_{\boldsymbol{\mu}^\top \hat{\boldsymbol{\mu}}_s > 0} \left(f(\hat{\boldsymbol{\mu}}_s) - f(-\hat{\boldsymbol{\mu}})\right) Q\left(\frac{1}{\sigma}\right) + f(-\hat{\boldsymbol{\mu}}_s) d\hat{\boldsymbol{\mu}}_s \\ &= \int_{\boldsymbol{\mu}^\top \hat{\boldsymbol{\mu}}_s > 0} f(\hat{\boldsymbol{\mu}}_s) d\hat{\boldsymbol{\mu}}_s \cdot Q\left(\frac{1}{\sigma}\right) + \int_{\boldsymbol{\mu}^\top \hat{\boldsymbol{\mu}}_s < 0} f(\hat{\boldsymbol{\mu}}_s) d\hat{\boldsymbol{\mu}}_s \cdot \left(1 - Q\left(\frac{1}{\sigma}\right)\right) \\ &= Q\left(-\frac{\sqrt{m}}{\sigma}\right) Q\left(\frac{1}{\sigma}\right) + Q\left(\frac{\sqrt{m}}{\sigma}\right)\left(1 - Q\left(\frac{1}{\sigma}\right)\right) \\ &= \left(1 - Q\left(\frac{\sqrt{m}}{\sigma}\right)\right) Q\left(\frac{1}{\sigma}\right) + Q\left(\frac{\sqrt{m}}{\sigma}\right)\left(1 - Q\left(\frac{1}{\sigma}\right)\right) \\ &= Q\left(\frac{1}{\sigma}\right) + Q\left(\frac{\sqrt{m}}{\sigma}\right) - 2Q\left(\frac{\sqrt{m}}{\sigma}\right) Q\left(\frac{1}{\sigma}\right).\end{aligned}$$

It completes the proof. □

E.5. Non-asymptotic Analysis

In Section 4 and Theorem 4.5, we showed that with infinitely many unlabeled samples, an L-layer linear attention model (for $L \geq 2$) can implement the predictor described in Theorem 4.4 with optimal $\boldsymbol{A}$ choice, achieving the classification error given by (11). In this section, we turn to the non-asymptotic setting where n is finite, and analyze the model's performance under this regime.

Theorem E.1. *Let the prompt $\boldsymbol{Z}$ be generated as described in Section 2.2, and consider an L-layer linear attention model with $L \geq 2$. Let $\hat{\boldsymbol{\mu}}_s$ be the SPI estimator defined in (SPI), and denote the optimal prediction as $y^\star_{\text{att-}L}(\boldsymbol{Z})$. Additionally, suppose that the number of labeled samples satisfies $m := np \geq d\sigma^2$. Then, there exists a universal constant $C > 0$ such that the classification error satisfies*

$$\mathbb{P}(y^\star(\boldsymbol{Z}) \neq y) \leq e^{C\sqrt{d/n}} \cdot Q\left(\frac{1}{\sigma}\right) + Q\left(\frac{\sqrt{m}}{\sigma}\right) + e^{-d}.$$

Proof. Recap from Proposition 4.1. For any L-layer attention model with $L \geq 2$, it can output

$$f_{\text{att-}L}(\boldsymbol{Z}) = \boldsymbol{x}^\top (\boldsymbol{X}^\top \boldsymbol{X}/n - \sigma^2 \boldsymbol{I}) \hat{\boldsymbol{\mu}}_s. \tag{33}$$

Let

$$\hat{y} = \operatorname{sgn}(f_{\text{att-}L}(\boldsymbol{Z}))$$

with $f_{\text{att-}L}(\boldsymbol{Z})$ defined in (33). Then we have

$$\mathbb{P}(y^\star(\boldsymbol{Z}) \neq y) \leq \mathbb{P}(\hat{y} \neq y).$$

Therefore, in the following, we focus on upper-bounding the classification error $\mathbb{P}(\hat{y} \neq y)$ corresponding to (33). Given that the optimal prediction under the form $\operatorname{sgn}(\boldsymbol{x}^\top \boldsymbol{A}\hat{\boldsymbol{\mu}}_s)$ is given by $\hat{y}_{\boldsymbol{\mu}\boldsymbol{\mu}^\top} := \operatorname{sgn}(\boldsymbol{x}^\top \boldsymbol{\mu}\boldsymbol{\mu}^\top \hat{\boldsymbol{\mu}}_s)$ (cf. Theorem 4.4), with its corresponding error presented in (11). To analyze the performance of $\hat{y}$, we study its difference from the prediction $\hat{y}_{\boldsymbol{\mu}\boldsymbol{\mu}^\top}$.

To begin with, let $\boldsymbol{g}_i = \boldsymbol{\xi}_i/\sigma \sim \mathcal{N}(0, \boldsymbol{I})$ and $\boldsymbol{g} = \sum_{i=1}^n \boldsymbol{\xi}_i/\sigma\sqrt{n} \sim \mathcal{N}(0, \boldsymbol{I})$. For simplicity, let $\boldsymbol{A} := \boldsymbol{X}^\top \boldsymbol{X}/n - \sigma^2 \boldsymbol{I}$. We get

$$\begin{aligned}
\boldsymbol{A} &= \frac{1}{n}\boldsymbol{X}^\top \boldsymbol{X} - \sigma^2 \boldsymbol{I} \\
&= \frac{1}{n}\left(\sum_{i=1}^n \boldsymbol{\mu}\boldsymbol{\mu}^\top + \boldsymbol{\mu}\boldsymbol{\xi}_i^\top + \boldsymbol{\xi}_i\boldsymbol{\mu}^\top + \boldsymbol{\xi}_i\boldsymbol{\xi}_i^\top\right) - \sigma^2 \boldsymbol{I} \\
&= \boldsymbol{\mu}\boldsymbol{\mu}^\top + \frac{\sigma}{\sqrt{n}}(\boldsymbol{\mu}\boldsymbol{g}^\top + \boldsymbol{g}\boldsymbol{\mu}^\top) + \sigma^2\left(\frac{\sum_{i=1}^n \boldsymbol{g}_i\boldsymbol{g}_i^\top}{n} - \boldsymbol{I}\right).
\end{aligned}$$

From the Laurent-Massart inequality (Laurent & Massart, 2000), we have that with probability at least $1 - e^{-t_1}$ (assuming $t_1 \geq d$),

$$\frac{1}{\sqrt{n}}\left\|\boldsymbol{\mu}\boldsymbol{g}^\top + \boldsymbol{g}\boldsymbol{\mu}^\top\right\| \leq \frac{2\|\boldsymbol{g}\|}{\sqrt{n}} \leq 6\sqrt{\frac{t_1}{n}}. \tag{34}$$

Additionally, from (Neopane, 2018), we have that with probability at least $1 - e^{-t_2}$ (assuming $t_2 \geq d$)

$$\left\|\frac{\sum_{i=1}^n \boldsymbol{g}_i\boldsymbol{g}_i^\top}{n} - \boldsymbol{I}\right\| \leq C_2 \cdot \sqrt{\frac{t_2}{n}}. \tag{35}$$

Define

$$\boldsymbol{\Delta} := \boldsymbol{A} - \boldsymbol{\mu}\boldsymbol{\mu}^\top = \frac{\sigma}{\sqrt{n}}(\boldsymbol{\mu}\boldsymbol{g}^\top + \boldsymbol{g}\boldsymbol{\mu}^\top) + \sigma^2\left(\frac{\sum_{i=1}^n \boldsymbol{g}_i\boldsymbol{g}_i^\top}{n} - \boldsymbol{I}\right).$$

Combining (34) and (35), we get with probability at least $1 - e^{-t}$ (for $t \geq d$)

$$\|\boldsymbol{\Delta}\| \leq C\sqrt{\frac{t}{n}}.$$

and therefore, with probability at least $1 - e^{-t}$

$$\boldsymbol{\mu}^\top \boldsymbol{A}\hat{\boldsymbol{\mu}}_s - \boldsymbol{\mu}^\top \boldsymbol{\mu}\boldsymbol{\mu}^\top \hat{\boldsymbol{\mu}}_s = \boldsymbol{\mu}^\top \boldsymbol{\Delta}\hat{\boldsymbol{\mu}}_s \leq \|\boldsymbol{\Delta}\| \cdot \|\hat{\boldsymbol{\mu}}_s\|.$$

Since $\hat{\boldsymbol{\mu}}_s \sim \mathcal{N}(\boldsymbol{\mu}, \sigma^2 \boldsymbol{m}\boldsymbol{I})$, similar to (34), with probability at least $1 - e^{-t_3}$ (assuming $d \leq t_3 \leq m/\sigma^2$), we can bound

$$\|\hat{\boldsymbol{\mu}}_s\| \leq 1 + \frac{\sigma}{\sqrt{m}}\|\boldsymbol{g}'\| \leq 1 + 3\sigma\sqrt{\frac{t_3}{m}} \leq 4.$$

Then consider a significantly large n (to ensure that $\|\boldsymbol{\Delta}\| \leq 1/8$). With probability at least $1 - e^{-\min(t,t_3)}$, we can bound

$$\left|\frac{\boldsymbol{\mu}^\top \boldsymbol{A}\hat{\boldsymbol{\mu}}_s}{\|\boldsymbol{A}\hat{\boldsymbol{\mu}}_s\|_{\ell_2}} - \frac{\boldsymbol{\mu}^\top \boldsymbol{\mu}\boldsymbol{\mu}^\top \hat{\boldsymbol{\mu}}_s}{\|\boldsymbol{\mu}\boldsymbol{\mu}^\top \hat{\boldsymbol{\mu}}_s\|_{\ell_2}}\right| \leq \frac{\|\boldsymbol{\Delta}\| \cdot \|\hat{\boldsymbol{\mu}}_s\|}{1 - \|\boldsymbol{\Delta}\| \cdot \|\hat{\boldsymbol{\mu}}_s\|} \leq C'\sqrt{\frac{t}{n}}.$$

Recall (29) from the proof of Theorem 4.4. The error for any given $\boldsymbol{\mu}, \hat{\boldsymbol{\mu}}_s$ is presented by

$$\mathbb{P}\left(\hat{y} \neq y \,\middle|\, \boldsymbol{\mu}, \hat{\boldsymbol{\mu}}_s\right) = Q\left(\frac{\boldsymbol{\mu}^\top \boldsymbol{A}\hat{\boldsymbol{\mu}}_s}{\sigma\left\|A\hat{\boldsymbol{\mu}}_s\right\|_{\ell_2}}\right).$$

Note that we have $Q(x - \delta) \leq e^{x\delta}Q(x)$ for $0 \leq \delta \ll x$. Then, for any $\boldsymbol{\mu}, \hat{\boldsymbol{\mu}}_s$ satisfying $\boldsymbol{\mu}^\top \hat{\boldsymbol{\mu}}_s > 0$, with probability at least $1 - e^{-\min(t,t_3)}$, we have

$$\begin{aligned}
\mathbb{P}\left(\hat{y} \neq y \,\middle|\, \boldsymbol{\mu}, \hat{\boldsymbol{\mu}}_s\right) &= Q\left(\frac{\boldsymbol{\mu}^\top \boldsymbol{A}\hat{\boldsymbol{\mu}}_s}{\sigma\left\|A\hat{\boldsymbol{\mu}}_s\right\|_{\ell_2}}\right) \\
&\leq e^{C''\sqrt{t/n}} \cdot Q\left(\frac{1}{\sigma}\right).
\end{aligned}$$

Combining all together, we obtain

$$\mathbb{P}\left(\hat{y} \neq y\right) \leq \mathbb{P}(\boldsymbol{\mu}^\top \hat{\boldsymbol{\mu}}_s > 0)\left(e^{C''\sqrt{t/n}} \cdot Q\left(\frac{1}{\sigma}\right) + e^{-t}\right) + \mathbb{P}(\boldsymbol{\mu}^\top \hat{\boldsymbol{\mu}}_s < 0)$$
$$\leq \left(e^{C''\sqrt{t/n}} \cdot Q\left(\frac{1}{\sigma}\right) + e^{-t}\right) + Q\left(\frac{\sqrt{m}}{\sigma}\right).$$

Choosing $t = d$ completes the proof. □

F. Additional Details on Tabular Experiments

Algorithm 1 LoopTabFM: Looping Tabular FM with Soft Pseudo-labels and Risk-aware Updates

Require: Dataset $\mathcal{D}_{\text{lab}}, \mathcal{D}_{\text{unlal}}$, looping iterations K

function `Looping`($\mathcal{D}_{\text{lal}}, \mathcal{D}_{\text{unlabel}}, K$)
  Base model/$\texttt{FM}_0 \leftarrow$ TabPFN-v2($\mathcal{D}_{\text{lab}}$)
  $\mathcal{D}_{\text{unlal}} \leftarrow \texttt{FM}_0(\mathcal{D}_{\text{unlab}})$ {Assign pseudo labels via $\hat{y}^{\text{soft}} \leftarrow \texttt{FM}_0(\boldsymbol{x} \in \mathcal{D}_{\text{unlab}})$.}
  $\texttt{FM}_{\text{best}} \leftarrow \texttt{FM}_0$
  $\mathcal{R}_{\text{val}} = \texttt{Val\_Risk}(\mathcal{D}_{\text{unlab}})$
  for Looping iteration $k = 1, \ldots, K$ **do**
    $\texttt{FM}_k \leftarrow$ TabPFN-v2($\mathcal{D}_{\text{lab}}, \mathcal{D}_{\text{unlab}}$)
    $\mathcal{D}_{\text{unlal}} \leftarrow \texttt{FM}_k(\mathcal{D}_{\text{unlab}})$ {Update pseudo labels via $\hat{y}^{\text{soft}} \leftarrow \texttt{FM}_k(\boldsymbol{x} \in \mathcal{D}_{\text{unlab}})$.}
    if $\texttt{Val\_Risk}(\mathcal{D}_{\text{unlab}}) < \mathcal{R}_{\text{val}}$ **then**
      $\texttt{FM}_{\text{best}} \leftarrow \texttt{FM}_k$
      $\mathcal{R}_{\text{val}} = \texttt{Val\_Risk}(\mathcal{D}_{\text{unlab}})$
    end if
  end for
  return $\texttt{FM}_{\text{best}}$
end function
function `Val_Risk`($\mathcal{D}_{\text{unlab}}$)
  return $\frac{1}{|\mathcal{D}_{\text{unlab}}|}\sum_i \min\left(\left|\hat{y}_i^{\text{soft}} - 1\right|, \left|\hat{y}_i^{\text{soft}} + 1\right|\right)$ {$\hat{y}_{\text{soft}}$ corresponds to the assigned soft label for feature in $\mathcal{D}_{\text{unlab}}$.}
end function

In this section, we provide additional details regarding the tabular experiments discussed in Section B.2. We propose the LoopTabFM algorithm with its details outlined in Algorithm 1. Suppose that we are given labeled $\mathcal{D}_{\text{lab}}$ and unlabeled $\mathcal{D}_{\text{unlab}}$ datasets during training. The overall workflow of the algorithm proceeds as follows:

1. **Base Model:** Train TabPFN on the labeled dataset $\mathcal{D}_{\text{lab}}$ and treat the resulting model as the base model (Loop-0). Its test accuracy is reported in Table 1.
2. **Pseudo-Label Assignment:** Using the current model (e.g., Loop-k), generate predictions for the unlabeled data $\mathcal{D}_{\text{unlab}}$. Assign soft pseudo-labels based on these predictions. Note that the model outputs are scalars (i.e., elements of $\mathbb{R}$) and can be interpreted as soft labels.
3. **Model Update:** Construct a new prompt that includes both labeled examples with their true labels and unlabeled examples with their assigned soft pseudo-labels. Fit the TabPFN to this combined prompt to obtain the updated model (Loop-$(k+1)$). Repeat from Step 2 until the maximum number of looping iterations is reached.

⋆ **Model Validation:** To improve the stability of the looping process, we introduce an additional validation step and retain the model with the lowest validation risk as the final (best) model. Specifically, suppose that the unlabeled data has been assigned soft pseudo-labels, i.e., $\mathcal{D}_{\text{unlab}} = \{(\boldsymbol{x}_i, \hat{y}_i^{\text{soft}})_{i=1}^n\}$. The validation risk is then computed over the pseudo labels as:

$$\texttt{Val\_Risk}(\mathcal{D}_{\text{unlab}}) = \frac{1}{n}\sum_{i\in[n]} \min\left(\left|\hat{y}_i^{\text{soft}} - 1\right|, \left|\hat{y}_i^{\text{soft}} + 1\right|\right),$$

which penalizes predictions that deviate from confident binary labels ± 1.